1 **MRGPRX4 is a novel bile acid receptor in cholestatic itch**

2 Huasheng Yu[1,2,3], Tianjun Zhao[1,2,3], Simin Liu[1], Qinxue Wu[4], Omar Johnson[4], Zhaofa

3 Wu[1,2], Zihao Zhuang[1], Yaocheng Shi[5], Renxi He[1,2], Yong Yang[6], Jianjun Sun[7],

4 Xiaoqun Wang[8], Haifeng Xu[9], Zheng Zeng[10], Xiaoguang Lei[3,5], Wenqin Luo[4*], Yulong

5 Li[1,2,3*]

6

7 [1]State Key Laboratory of Membrane Biology, Peking University School of Life

8 Sciences, Beijing 100871, China

9 [2]PKU-IDG/McGovern Institute for Brain Research, Beijing 100871, China

10 [3]Peking-Tsinghua Center for Life Sciences, Beijing 100871, China

11 [4]Department of Neuroscience, Perelman School of Medicine, University of

12 Pennsylvania, Philadelphia, PA 19104, USA

13 [5]Department of Chemical Biology, College of Chemistry and Molecular Engineering,

14 Peking University, Beijing 100871, China

15 [6]Department of Dermatology, Peking University First Hospital, Beijing Key Laboratory

16 of Molecular Diagnosis on Dermatoses, Beijing 100034, China

17 [7]Department of Neurosurgery, Peking University Third Hospital, Peking University,

18 Beijing, 100191, China

19 [8]State Key Laboratory of Brain and Cognitive Science, CAS Center for Excellence in

20 Brain Science and Intelligence Technology (Shanghai), Institute of Biophysics,

21 Chinese Academy of Sciences, Beijing, 100101, China

22 [9]Department of Liver Surgery, Peking Union Medical College Hospital, Chinese

23 Academy of Medical Sciences and Peking Union Medical College, Beijing 100730,

24 China

25 [10]Department of Infectious Diseases, Peking University First Hospital, Beijing 100034,

26 China

27 *Manuscript correspondence:

28 Yulong Li (yulongli@pku.edu.cn) & Wenqin Luo (luow@pennmedicine.upenn.edu)

29

35

36

37

38

39

40

41

42

43   **Abstract:**

44   Patients with liver diseases often suffer from chronic itch or pruritus, yet the

45   itch-causing pruritogen(s) and their cognate receptor(s) remain largely elusive. Using

46   transcriptomics and GPCR activation assays, we found that an orphan, primate

47   specific MRGPRX4 is expressed in human dorsal root ganglia (hDRG) and selectively

48   activated by bile acids. *In situ* hybridization and immunohistochemistry revealed that

49   MRGPRX4 is expressed in ~7% of hDRG neurons and co-localizes with HRH1, a

50   known itch-inducing GPCR. Bile acids elicited a robust Ca^{2+} response in a subset of

51   cultured hDRG neurons, and intradermal injection of bile acids and an MRGPRX4

52   specific agonist induced significant itch in healthy human subjects. Surprisingly,

53   application of agonist for TGR5, a known sequence conserved bile acid receptor

54   previously implicated in cholestatic itch, failed to elicit Ca^{2+} response in cultured

55   hDRG neurons, nor did it induce pruritus in human subjects. *In situ* hybridization and

56   immunostaining results revealed that hTGR5 is selectively expressed in satellite glial

57   cells, unlike mTGR5 (in mouse DRG neurons), likely accounting for the inter-species

58   difference functionally. Finally, we found that patients with cholestatic itch have

59   significantly higher plasma bile acid levels compared to non-itchy patients and the bile

60   acid levels significantly decreased after itch relief. This elevated bile acid level in itchy

61   patients is sufficient to activate MRGPRX4. Taken together, our data strongly suggest

62   that MRGPRX4 is a novel bile acid receptor that likely underlies cholestatic itch,

63   providing a promising new drug target for anti-itch therapies.

64

INTRODUCTION

Chronic itch, or pruritus, is a severe and potentially debilitating clinical feature associated with many dermatological and systemic conditions[1], severely affecting quality of life and potentially leading to lassitude, fatigue, and even depression and suicidal tendencies[2]. The most well-characterized itch receptors are the H1 and H4 histamine receptors (HRH1 and HRH4)[3]. Although antihistamines, which act by inhibiting histamine receptors, are generally effective at relieving itch symptoms induced by inflammation and allergens, these compounds are usually ineffective at treating chronic itch caused by systemic diseases and most skin disorders. To date, no effective treatment is available for treating histamine-resistant itch[2].

A high percentage of patients with systemic liver failure develop itch with cholestatic symptoms[4]. For example, the prevalence of itch is as high as 69% among patients with primary biliary cirrhosis, and severe itch is an indication for liver transplantation[5]. Moreover, itch occurs in more than half of pregnant woman with intrahepatic cholestasis of pregnancy, a condition that has been associated with an increased risk of preterm delivery, perinatal mortality, and fetal distress[6].

Several medications have been tested for treating cholestatic itch, including ursodeoxycholic acid (UDCA), cholestyramine, and rifampicin; however, these compounds either are ineffective or induce severe side effects[5]. Therefore, safe and effective treatments for cholestatic itch are urgently needed, and identifying the underlying molecular mechanisms—particularly the receptor and ligand—is the essential first step.

Although the link between cholestasis and itch was first described more than

88   2000 years ago[7], the detailed mechanisms underlying cholestatic itch remain

89   unidentified. To date, a handful of molecules have been proposed as the pruritogens

90   that mediate cholestatic itch, including bile acids, bilirubin, lysophosphatidic acid,

91   autotaxin, and endogenous opioids[4]. With respect to the cognate receptor for the

92   pruritogen, a few receptors have been proposed, albeit based primarily on rodent

93   models. For example, the membrane-bound bile acid receptor TGR5 has been

94   reported to mediate bile acid□induced itch in mice[8,9]. However, a recent study found

95   that administering TGR5-selective agonists failed to elicit an itch response in mouse

96   models of cholestasis[10], raising doubts regarding whether TGR5 is indeed the

97   principal mediator for cholestatic itch. Recently, Meixiong et al. reported that Mrgpra1

98   and MRGPRX4 (in mice and humans, respectively) can be activated by bilirubin, a

99   compound that serves as one of the pruritogens in cholestatic itch in mice[11].

100   Nevertheless, the precise molecular mechanism that underlie cholestatic itch in

101   humans remains to be determined.

102   We specifically focused our search on genes that are selectively expressed in the

103   human dorsal root ganglia (DRG), where the cell bodies of primary itch-sensing

104   neurons are located. Our search revealed a novel ligand-receptor pair comprised of

105   bile acids (the ligand) and the receptor MRGPRX4. Moreover, we found that

106   MRGPRX4 is expressed selectively in a small subset of neurons in the human DRG,

107   and bile acids directly trigger intracellular Ca^{2+} increase in these neurons. In addition,

108   intradermal injection of both bile acids and the MRGPRX4-specific agonist nateglinide

109   induce detectable itch in human subjects, and this bile acid-induced itch is

110   histamine-independent. Surprisingly, application of agonist for TGR5, a known

111   sequence conserved bile acid receptor previously implicated in cholestatic itch, failed

112   to elicit Ca^{2+} response in cultured hDRG neurons, nor did it induce pruritus in human

113   subjects. In situ hybridization and immunostaining results revealed that unlike

114   mTGR5 expressing in mouse DRG neurons, hTGR5 is selectively expressed in

115   satellite glial cells, likely accounting for the inter-species difference functionally.

116   Finally, we found that plasma bile acid levels are well correlated with itch sensation in

117   cholestatic patients and that this elevated bile acid level is sufficient to activate

118   MRGPRX4. Taken together, our results provide compelling evidence that the

119   ligand-receptor pair of bile acids and MRGPRX4 is likely to be one of the critical

120   mediators for human cholestatic itch.

121

122   **RESULTS**

123   ***MRGPRX4 is activated by bile extract***

124   DRG neurons are primary somatosensory neurons that express a variety of receptors

125   and ion channels for detecting both extrinsic and intrinsic stimuli[12]. To identify a

126   receptor in mediating cholestatic itch in human, we reason that this candidate

127   receptor could be expressed in human DRG neurons and activated by bile extracts.

128   Since the majority of itch receptors identified to date belong to the G protein☐coupled

129   receptor (GPCR) superfamily[13], we analyzed two published transcriptomics datasets

130   compiled from a variety of human tissues[14,15], specifically focusing on GPCRs.

131   Among the 332 transcripts that are enriched in the human DRG (Table S1), we

132   identified the following seven highest-enriched orphan GPCRs: GPR149, MRGPRX4,

133   GPR139, GPR83, MRGPRE, MRGPRX1, and MRGPRD[16,17] (**Fig. 1a and Table S2**).

134   Next, we cloned and expressed these candidate receptors in HEK293T cells

135   (**Supplementary Fig. 1a, b**), finding that all seven receptors were expressed at the

136   plasma membrane (**Supplementary Fig. 1b**). We measured the activation of each

137   receptor by bovine bile extract using two reporter assays, the Gs-dependent

138   luciferase assay[18] and the Gq-dependent TGFα shedding assay[19] (**Fig. 1b,c**). No

139   signal was detected with the Gs-dependent luciferase assay (**Fig. 1b**). Interestingly,

140   bile extract elicited a significant increase in reporter activity in cells expressing

141   MRGPRX4 measured using the TGFα shedding assay, but had no effect on cells

142   expressing the other six GPCRs (**Fig. 1c**). These results suggest that MRGPRX4 is

143   activated by one or more compounds present in bile extract, and that MRGPRX4

144   likely signals through the Gq but not the Gs pathway. Further experiments revealed

145   that bovine, porcine, and human bile extract activate MRGPRX4 to a similar extent in

146   a dose-dependent manner (**Fig. 1d**); in contrast, extracts obtained from bovine brain,

147   spleen, heart, kidney, and liver tissues induced no detectable signal on

148   MRGPRX4-expressing cells (**Fig. 1e**). Taken together, these results suggest that

149   MRGPRX4 is potently activated by bile extract and active compound(s) is/are highly

150   enriched in bile extract.

151

152   ***Identifying which in bile extract activate MRGPRX4***

153   Next, to identify the component(s) in bovine bile extract that activate(s) MRGPRX4,

154 we separated the extract into six fractions using silica gel column chromatography

155 (**Fig. 2a**). Each fraction was then applied to MRGPRX4-expressing HEK293T cells,

156 and MRGPRX4 activation was measured using the TGFα shedding assay. Among the

157 six fractions tested, fraction 4 caused the strongest activation of MRGPRX4, whereas

158 fractions 1 and 6 caused the weakest activity (**Fig. 2b**), indicating that the active

159 component(s) are mainly present in fraction 4. Mass spectrometry of fractions 4 and 6

160 revealed a peak enriched specifically in fraction 4 (**Fig. 2c**); this peak corresponded to

161 ions with an m/z value of 410.3265 in the positive ion mode and was annotated to

162 prostaglandin F2α diethyl amide and/or dihydroxy bile acids. Further experiments

163 using ^{1}H-NMR revealed that two pure dihydroxy bile acids—deoxycholic acid (DCA)

164 and chenodeoxycholic acid (CDCA)—produced peaks that were identical to the

165 peaks in fraction 4 (**Fig. 2d**); other fractions that only weakly activated MRGPRX4

166 also contained characteristic peaks of bile acids as shown by ^{1}H-NMR

167 (**Supplementary Fig. 2**). These results suggest that DCA and/or CDCA are enriched

168 in the active fraction of bile extract and may be the key compounds that activate

169 MRGPRX4.

170

171 ***Characterization of bile acids: MRGPRX4 activation and the downstream***

172 ***signaling***

173 To further characterize the efficacy and potency of DCA, CDCA, other bile acids, and

174 their derivatives in activating MRGPRX4, we systematically measured their ability to

175 activate MRGPRX4 in HEK293T cells, using TGFα shedding assay and FLIPR

176 (fluorescent imaging plate reader) Ca^{2+} assay. All of the bile acids tested activated

177 MRGPRX4 to some extent; DCA had the highest potency measured with both assays,

178 with an EC_{50} value of 2.7 μM and 2.6 μM in the TGFα shedding and FLIPR assays,

179 respectively; cholic acid (CA), CDCA, and lithocholic acid (LCA)—three close analogs

180 of DCA—were less potent (**Fig. 3a-c**). Based on the structural differences between

181 DCA and the less potent bile acids, we reasoned that hydroxylation at position of R1

182 and/or R2, as well as taurine/glycine conjugation at position R3, is important for

183 specific bile acids to activate MRGPRX4 (**Fig. 3c**).

184 Next, we examined the potential signaling events downstream of bile

185 acid-induced MRGPRX4 activation by measuring intracellular Ca^{2+} concentration

186 ($[Ca^{2+}]_i$) in MRGPRX4-expressing HEK293T cells loaded with Fluo-8 AM, a

187 fluorescent Ca^{2+} indicator. We found that DCA, CA, CDCA, and LCA induced a robust

188 fluorescence response in these cells (**Fig. 3d-f**), and pretreating the cells with the

189 phospholipase C inhibitor U73122 significantly reduced the DCA-evoked Ca^{2+} signals;

190 in contrast, the Gβγ inhibitor gallein had no effect on DCA-evoked signaling (**Fig.**

191 **3g-h**). Taken together, these results indicate that a Gq-dependent signaling pathway

192 involving phospholipase C is downstream to MRGPRX4 activation by bile acids.

193 Interestingly, even though MRGPRX1, MRGPRX2, and MRGPRX3 are close

194 analogs of MRGPRX4, none of these receptors was activated by bile acids, even at

195 100 μM concentration (**Supplementary Fig. 3a-e**). We therefore investigated the

196 putative ligand-binding sites in MRGPRX4 by comparing the primary amino acid

197 sequence of MRGPRX4 with these three analogs (**Fig. 3i**). We identified amino acid

198 residues that are conserved in MRGPRX1, MRGPRX2, and MRGPRX3 but not in

199 MRGPRX4 and mutated these residues, once per time, to an alanine residue in

200 MRGPRX4. We found that mutating amino acids 159, 180, and 235 reduced the

201 receptor's affinity for DCA (**Fig. 3j**), without affecting trafficking to the cell membrane

202 (**Fig. 3k**); thus, these three sites may play a critical role in the binding of bile acids to

203 MRGPRX4. In addition, we examined whether mouse and/or rat Mrgpr family

204 members also respond to bile acids. Intriguingly, bile acids failed to activate any

205 mouse or rat Mrgpr members tested (**Supplementary Fig. 3g-h**), suggesting that the

206 ability of MRGPRX4 to sense bile acids may be a new functional addition during

207 evolution.

208

209 ***A subset of human itch-related DRG neurons express MRGPRX4 and respond***

210 ***to bile acids***

211 Next, we examined endogenous expression pattern of MRGPRX4 in hDRGs. We

212 performed *in situ* hybridization using a digoxigenin-labeled riboprobe against

213 *MRGPRX4* mRNA, and found that *MRGPRX4* mRNA is expressed in only ~6-8% of

214 hDRG neurons (**Fig. 4a, c**); similar results were obtained with immunofluorescence

215 using an MRGPRX4-specific antibody (**Fig. 4b, c** and **Supplementary Fig. 4**).

216 Morphologically, these MRGPRX4-expressing neurons are small-diameter neurons,

217 with a diameter of approximately 50 μm, which is similar to small-diameter neurons

218 that express the neurotrophic tyrosine kinase receptor type 1 (TrkA) (**Fig. 4d**),

219 suggesting a function in nociception and/or pruriception[20].

220   To further characterize the molecular profile of these MRGPRX4-positive hDRG

221   neurons, we performed triple-labeling of MRGPRX4 and two additional molecular

222   markers using RNAscope *in situ* hybridization (**Fig. 4e**). Our analysis revealed

223   that >90% of MRGPRX4-positive neurons also express the histamine receptor HRH1,

224   a well-characterized itch receptor in humans[21], and TRPV1 (transient receptor

225   potential cation channel subfamily V member 1) (**Fig. 4f-g**), which functions

226   downstream of Mrgprs and histamine receptors[22,23]. Interestingly, the majority of

227   MRGPRX4-expressing neurons also co-express $Na_v1.7$ voltage-gated sodium

228   channel, the peptidergic marker CGRP (calcitonin gene-related peptide), and

229   TrkA[24,25] (**Fig. 4f-g**). These results suggest that MRGPRX4 is specifically expressed

230   in a subset of small diameter peptidergic hDRG neurons.

231   Next, we tested whether MRGPRX4 in DRG neurons can be activated by bile

232   acids. Because bile acids failed to induce a detectable Ca^{2+} signal in cultured rat

233   DRG neurons (**Supplementary Fig. 5**), we expressed the human MRGPRX4 in

234   cultured rat DRG neurons. Bile acids triggered a robust Ca^{2+} response in

235   MRGPRX4-expressing rat DRG neurons (**Supplementary Fig. 5**), indicating that

236   MRGPRX4 expressed in rat DRG neurons mediates the bile acid☐induced activation.

237   Consistent with our finding that DCA is a more potent agonist of MRGPRX4 than CA,

238   DCA induced a significantly larger Ca^{2+} response and activated a larger number of

239   MRGPRX4-expressing rat DRG neurons than CA (**Supplementary Fig. 5**).

240   Next, we asked whether hDRG neurons can also be activated by bile acids.

241   Application of DCA induced a robust fluorescence increase in a subset (~6%) of these

242   hDRG neurons loaded with Fluo-8 AM; this percentage of DCA-responsive cells is

243   similar to the percentage of MRGPRX4-expressing cells measured with *in situ*

244   hybridization (**Fig. 4a, c**). Moreover, the less potent MRGPRX4 agonist CA also

245   induced a response, albeit much weaker than DCA (**Fig. 4h** and **Supplementary Fig.**

246   **6**). In addition, nearly all (~90%) of DCA-responsive hDRG neurons were

247   capsaicin-sensitive, and approximately one-third of DCA-responsive neurons also

248   responded to histamine (**Fig. 4j**). Together, our results indicate that expression of

249   MRGPRX4 is sufficient to render bile acid sensitivity of primary somatosensory

250   neurons.

251

252   ***Pharmacological activation of MRGPRX4 triggers itch sensation in human***

253   ***subjects***

254   Given the specific expression pattern of MRGPRX4 in a subset of hDRG neurons,

255   and the known role of Mrgpr family members in mediating itch sensation, we next

256   asked whether pharmacologically activating MRGPRX4 could trigger itch sensation in

257   human subjects. We recruited healthy volunteers and performed a double-blind skin

258   itch test, in which each subject received a 25-μl intradermal injection of the test

259   compounds or vehicle in four separate sites on both forearms (**Fig. 5a1, inset**), after

260   which the subject was asked to rank the itch sensation at each injection site using a

261   generalized labeled magnitude scale (LMS)[26]. Interestingly, the pharmacological

262   MRGPRX4 specific agonist nateglinide, a previously reported MRGPRX4 agonist[27],

263   (**Supplementary Fig. 3f**) —but not vehicle—induced a robust itch sensation in

264   healthy subjects (**Fig. 5a1, a2**). These results show that activation of MRGPRX4 is

265   sufficient to trigger itch sensation in humans, suggesting that MRGPRX4 is a human

266   itch receptor.

267

268   ***Bile acid◻induced itch in humans is both histamine- and TGR5-independent***

269   Previous studies have implicated that bile acids could induce itch in human[28,29]. Here,

270   we systematically test pruritic effect of bile acids on human and whether bile aicd-

271   induced itch shows some features similar to that of cholestatic itch[17]. We found that

272   500 μg (25 μl) of DCA induced a significant itch sensation that peaked within 5 min

273   and declined slowly over time; in contrast, control injections with vehicle did not

274   induce an itch response (**Fig. 5a1, a2**). Moreover, itch intensity induced by DCA was

275   in a dose-dependent manner (**Fig. 5b1, b2**). We also found that less potent

276   MRGPRX4 agonists, including CA, CDCA, taurochenodeoxycholic acid (TCDCA),

277   and LCA, also induced a weaker—albeit still significant—itch sensation (**Fig. 5c1, c2**).

278   Given that antihistamines are largely ineffective for treating cholestatic itch[4], we

279   tested whether itch induced by bile acids can be blocked by antihistamines. We found

280   that pretreating subjects with an antihistamine prevented histamine-induced itch but

281   had no effect on DCA-induced itch (**Fig. 5d1, d2**), suggesting that itch induced by bile

282   acids does not involve histamine signaling. Taken together, these results indicate that

283   bile acids trigger an itch sensation with features similar to cholestatic itch.

284   In mice, the membrane bile acid receptor TGR5 has been reported to mediate

285   bile acid◻induced itch[8,9]. To test whether bile acid-induced itch in human is also

286   mediated by TGR5, we chose a non-bile acid TGR5 agonist compound 15[30], which is

287   nearly 70-fold more potent than DCA in activating human TGR5 and does not activate

288   human MRGPRX4 (**Fig. 6b, c**). Intradermal injections of 10 µg (25µl) of compound 15

289   did not induce detectable itch in humans, whereas DCA, as the positive control,

290   induced significant itch (**Fig. 6a1, a2, d**). These results suggest that TRG5 is not the

291   receptor mediating bile acid-induced itch. Furthermore, we examined the expression

292   of TGR5 in the human, monkey, and mouse DRG tissues. Very surprisingly, although

293   the amino acid sequence of TGR5 is relatively conserved between rodents and

294   primates (**Supplementary Fig. 7a**), we found the different expression pattern of

295   TGR5 in DRG tissues. In human and monkey, both *in situ* hybridization and

296   immunostaining revealed that TGR5 is highly expressed in satellite glial cells

297   surrounding DRG neurons but not the primary sensory neurons (**Fig. 6e-i and**

298   **Supplementary Fig. 7**), while in mouse, the same *in situ* probe and antibody

299   detected the expression of TGR5 in mouse DRG neurons (**Fig. 6f, h and**

300   **Supplementary Fig. 7c**), similar to the previous publication[8,9]. These results

301   revealed an interesting species difference in TGR5 expression and function between

302   mouse and primate. Taken together, our results demonstrate that the function of

303   TGR5 in human somatosensory system is different from that in mouse, and TGR5 is

304   not the receptor for mediating bile acid-induced itch in human.

305

306   ***The elevated levels of bile acids in cholestatic itchy patients are sufficient to***

307   ***activate MRGPRX4***

308   Lastly, to investigate whether bile acids are the pruritogens under pathological

309   conditions, we collected plasma samples from patients with liver or skin diseases and

310   measured the concentration of 12 major bile acids using HPLC-MS/MS (**Fig. 7a and**

311   **Supplementary Fig. 8a**). We found that glycine- and taurine-conjugated primary bile

312   acids, including glycocholic acid (GCA), taurocholic acid (TCA),

313   glycochenodeoxycholic acid (GCDCA), and TCDCA are the major bile acids present

314   in cholestatic patients (**Fig. 7a**), consistent with previously published results[31-33].

315   Compared to itchy patients with liver diseases, non-itchy patients had significantly

316   higher levels of total bile acids (defined here as the sum of the 12 bile acids shown in

317   **Fig. 7a**) (**Fig. 7a, b**). The level of total plasma bile acids in the itchy patients with skin

318   diseases was barely detectable and significantly lower than the itchy patients with

319   liver diseases. Among the 12 bile acids measured, the ones with the largest

320   differences between the patients with itch and those without itch were for GCA,

321   GCDCA, TCA, and TCDCA (**Fig. 7a, b**), suggesting that these four bile acids play key

322   roles in mediating chronic itch under pathological conditions. Indeed, intradermal

323   injections of TCDCA caused significant itch in healthy subjects (**Fig. 5c1, c2**). For

324   DCA, the most potent ligand for MRGPRX4 among all tested bile acids, we did not

325   see the significant difference between itchy and non-itchy patients with liver diseases

326   (**Fig. 7a**), suggesting it is not the major contributor for cholestatic itch under

327   pathological conditions. More importantly, although bile acid levels vary among itchy

328   patients with liver diseases both from our data (**Fig. 7a, b**) and previously reported

329   results[32-34], we found that the total plasma bile acids, as well as the individual levels of

330   GCDCA, TCDCA, TCA, and GCA, significantly decreased in 11 out of 13 patients

331   following itch relief (**Fig. 7c, d** and **Supplementary Fig. 8c**). Taken together, these

332   results suggest that high levels of bile acids are well correlated with itchy symptom in

333   patients with liver diseases and that bile acids—particularly GCDCA, TCDCA, TCA,

334   and GCA— could be main metabolites triggering cholestatic itch.

335   Next, we examined whether combinations of bile acids at pathologically relevant

336   levels are sufficient to activate MRGPRX4. We prepared mixtures of bile acids similar

337   to the plasma/serum levels in healthy subjects ("healthy mix") or in patients with liver

338   diseases and itch ("liver itch mix"), which are estimated based on previously

339   published data[31,35] and our quantification results (**Fig. 7a**). These mixtures were then

340   applied to MRGPRX4-expressing HEK293T cells while performing Ca^{2+} imaging. We

341   found that the "liver itch mix" but not "healthy mix" induced a significant Ca^{2+} signal

342   (**Fig. 7e, f**), suggesting that pathological relevant level of bile acids is sufficient to

343   activate MRGPRX4.

344   Recently, Meixiong et al. reported that MRGPRX4 can also be activated by

345   bilirubin, which is another potential pruritogen for triggering cholestatic itch[11]. We

346   therefore compared bilirubin and DCA with respect to binding and activating

347   MRGPRX4. We found that compared to bile acids, bilirubin is a less potent, partial

348   agonist of MRGPRX4 (**Supplementary Fig. 9a**). Given the structural differences

349   between bilirubin and DCA, we then tested whether bilirubin is an allosteric modulator

350   of MRGPRX4. Indeed, we found that bilirubin can potentiate the activation of

351   MRGPRX4 by DCA (**Supplementary Fig. 9b**), and—conversely—DCA potentiate the

352 activation of MRGPRX4 by bilirubin (**Supplementary Fig. 9c**). Moreover, we found

353 that both total bilirubin and conjugated bilirubin levels were significantly higher in itchy

354 patients with liver diseases compared to non-itchy patients (**Supplementary Fig. 9d**)

355 and plasma bilirubin levels decreased significantly after itch relief (**Supplementary**

356 **Fig. 9e**). Compare to total bilirubin, total bile acids show better correlation with itch

357 intensity (measured using a self-report numerical rating scale[36]) (**Supplementary Fig.**

358 **9f**). Taken together, these results suggest that bile acids are the major pruritogens in

359 MRGPRX4-mediated cholestatic itch and bilirubin facilitates the activation of

360 MRGPRX4 by bile acids and may also contribute to cholestatic itch in pathological

361 conditions.

362

363 **DISCUSSION**

364 Here, we report that MRGPRX4 is a novel GPCR that fits with the criteria we set for

365 identifying putative receptor in mediating cholestatic itch. MRGPRX4 is selectively

366 expressed in a small subset of human DRG neurons. Bile acids triggered a robust

367 Ca^{2+} response in a subset of hDRG neurons as well as rat DRG neurons expressing

368 MRGPRX4 exogenously. Both bile acids and an MRGPRX4-specific agonist induce

369 itch in human. Bile acid-induced itch in human is histamine independent, which is

370 consistent with antihistamines are largely ineffective for treating cholestatic itch.

371 Surprisingly, application of agonist for TGR5 failed to elicit Ca^{2+} response in cultured

372 hDRG neurons, nor did it induce pruritus in human subjects. The expression pattern

373 of TGR5 is different between mouse and human. hTGR5 is selectively expressed in

374 satellite glial cells, while mTGR5 is expressed in DRG neurons, likely accounting for

375 the inter-species difference functionally. We also found that plasma levels of bile

376 acids were well correlated with itchy patients with liver diseases. Importantly, a

377 mixture of bile acids with components and concentrations similar to that of cholestatic

378 itchy patients—but not healthy volunteers—was sufficient to activate MRGPRX4. Our

379 data indicate bile acids are the major pruritogens in MRGPRX4-mediated cholestatic

380 itch and bilirubin facilitates the activation of MRGPRX4 by bile acids and may also

381 contribute to cholestatic itch in pathological conditions. Based on our results, we

382 propose a new working model for cholestatic itch (**Fig. 7g**): patients with cholestasis

383 usually display increased plasma levels of bile acids and bilirubin, which are

384 precipitated in the skin and activate MRGPRX4 receptors in itch-related primary fibers,

385 thereby triggering itch in these patients. Our results exclude TGR5 as a primary itch

386 receptor in human, and the broad expression of TGR5 in satellite glial cells implies a

387 more general function which remains to be determined in the future.

388 Here, we provide important evidence that MRGPRX4 is sufficient for mediating

389 bile acid□induced itch, and thus should play an important role in cholestatic itch.

390 Since specific antagonist for MRGPRX4 is currently unavailable, we could not

391 determine whether MRGPRX4 is necessary for bile acids induced itch in human.

392 Future studies will be designed to further examine the role of MRGPRX4 in

393 cholestatic itch using to-be-developed pharmacological and/or human genetic

394 approaches. For example, several single-nucleotide polymorphisms (SNPs) have

395 been identified in the human *MRGPRX4* gene[37], and it would be interesting to screen

396   for loss-of-function and gain-of-function *MRGPRX4* variants. Characterizing the

397   relationship between these variants and itch intensity in cholestatic patients and

398   healthy subjects with bile acid☐induced itch could help to further delineate the

399   relationship between MRGPRX4 activity and cholestatic itch. These experiments will

400   also help to determine whether MRGPRX4 is the main molecular receptor for

401   mediating cholestatic itch, or whether other GPCRs[4], such as lysophosphatidic acid

402   receptors and serotonin receptors also play roles in cholestatic itch.

403   Our current understandings about mechanisms underlying somatosensation in

404   the mammalian system are mainly derived from studies of rodents. Despite the great

405   value and insights we gained using rodent models, notable failures have happened in

406   translating results obtained in rodents into effective and safe clinical treatments in

407   human[38-41]. The bile acid receptors we study here is a great example demonstrating

408   the species differences between rodent and human somatosensory systems.

409   Although TGR5, a bile acid membrane receptor, was previously reported to be

410   expressed in mouse DRG neurons and mediate bile acid☐induced itch in mice[8,9], our

411   expressing characterizations as well as functional assays revealed that TGR5 is not

412   expressed in human DRG neurons and doesn't directly mediate itch sensation in

413   human. Instead, primate MRGPRX4 gains the novel function of bile acid sensitivity

414   during evolution. Therefore, it is crucial to study and validate the mechanism of

415   cholestatic chronic itch and develop the correspondent treatment within the context of

416   human physiology.

417   Recently, Meixiong et al. reported that mouse Mrgpra1 and human MRGPRX4

418 can be activated by bilirubin, suggesting that bilirubin may serve as a pruritogen in

419 cholestatic itch[11]. Bilirubin, a yellow compound that causes the yellow discoloration in

420 jaundice, has not been considered a likely candidate pruritogen though, because the

421 clinical observation that itch often precedes the appearance of jaundice, particularly in

422 patients with intrahepatic cholestasis of pregnancy (ICP)[42] and patients with primary

423 biliary cirrhosis[7]. Our results suggest that bilirubin is a partial agonist of MRGPRX4

424 and may potentiate the activation of MRGPRX4 by bile acids. This notion is

425 consistent with our finding that the correlation between bile acid levels and itch

426 intensity is stronger than the correlation between bilirubin levels and itch intensity.

427 Based on these findings, we propose that bile acid is the major contributor to

428 cholestatic itch, and bilirubin serves to increase bile acid□induced cholestatic itch

429 under pathological conditions.

430 In summary, we found that the membrane-bound GPCR MRGPRX4 is a novel bile

431 acid receptor and may serve as an important molecular mediator of chronic itch in

432 patients with systemic liver diseases. Our results suggest that MRGPRX4 is a

433 promising molecular target for developing new treatments to alleviate devastating

434 chronic itch in these patients.

435

436 **Data availability statement**

437 The data that support the findings of this study are available from the corresponding

438 author upon request. All figures have associated raw data. There is no restriction

439 regarding data availability.

440

Conflict of interest

442 The authors declare no competing interests.

443

444

445

446

447

448 **Figures and legends**

449 **Fig. 1 MRGPRX4 is activated by bile extract.**

450 (**a**) Flow chart for the strategy used to identify orphan GPCRs enriched in human

451 DRG. Transcriptome analysis of DRG and other tissues (trigeminal ganglia, brain,

452 colon, liver, lung, skeletal muscle, and testis) revealed 332 transcripts with high

453 expression in the DRG. The top seven orphan GPCRs are listed. See also

454 Supplementary Tables S1 and S2. Gene expression data were obtained from Flegel

455 et al. *PLoS One*, 2013 & 2015.

456 (**b** and **c**) Activation of MRGPRX4 by bovine bile extract. The diagrams at the top

457 depict the reporter gene assays used to measure GPCR activation via Gs-dependent

458 (**b**) and Gq-dependent (**c**) pathways. The seven GPCRs identified in (**a**) were tested,

459 revealing that MRGPRX4-expressing HEK293T cells are activated by bile extract via

460 the Gq-dependent pathway. Forskolin and TPA were used as positive controls for

461 activating Gs- and Gq-dependent signaling, respectively. The responses obtained

462   from the tested GPCRs were normalized to the responses induced by respective

463   positive controls. As positive controls for detecting GPCR activation, separate cells

464   were transfected with ADRB1 and stimulated with 10 µM norepinephrine (NE) (**b**) or

465   transfected with HRH1 and stimulated with 10 µM histamine (His) (**c**). "HEK (only)"

466   refers to non-transfected cells. n = 3 experiments performed in triplicate.

467   (**d**) Concentration-response curve for the activation of MRGPRX4 by bovine bile

468   extract, porcine bile extract, and human bile measured using the TGFα shedding

469   assay. The bovine and porcine bile extract solutions were diluted 1 :10 from a 100 µ

470   g/ml stock solution, and the human bile solution was diluted 1:10 from crude human

471   bile. n = 2 experiments performed in triplicate.

472   (**e**) MRGPRX4 is activated selectively by bovine, porcine, and human bile extracts,

473   but not by bovine brain, spleen, heart, kidney, or liver tissue extracts. The data for

474   porcine and human bile are reproduced from (**d**). n = 2 experiments performed in

475   triplicate. Student's *t*-test, *$p < 0.05$, ***$p < 0.001$, and n.s. not significant ($p > 0.05$).

476

477   **Fig. 2 Identification of the active components in bile extract that activate**

478   **MRGPRX4.**

479   (**a**) Flow chart depicting the strategy for isolating and identifying candidate MRGPRX4

480   ligands in bovine bile extract. F1 through F6 indicate the six fractions used in

481   subsequent experiments.

482   (**b**) Activation of MRGPRX4 by bile extract fractions F1 through F6; fraction F4 has

483   the highest activity. The data represent one experiment performed in triplicate.

484   Student's *t*-test, **$p < 0.01$. ***$p < 0.001$ versus fraction F4.

485   (**c**) MS analysis of fractions F4 and F6 (which showed high and weak activity,

486   respectively). The selectively enriched peak in fraction F4 at molecular weight

487   410.3265 corresponds to the bile acids DCA and CDCA.

488   (**d**) ^{1}H-NMR analysis of fractions F4 and F6 using purified DCA and CDCA as

489   controls.

490

491   **Fig. 3 Functional characterization and molecular profiling of bile acids as**

492   **ligands for MRGPRX4.**

493   (**a-c**) Dose-dependent activation of MRGPRX4 by various bile acids and their

494   derivatives. MRGPRX4 activation was measured using the TGFα shedding assay (**a**)

495   or the FLIPR assay (**b**, see methods) in MRGPRX4-expressing HEK293T cells; n = 1

496   experiment performed in triplicate. The general structure of the bile acids and

497   derivatives is shown in (**a**), and the respective potencies of the bile acids/derivatives

498   are listed in (**c**).

499   (**d-f**) Activation of MRGPRX4 by various bile acids in cells loaded with the Ca^{2+}

500   indicator Fluo-8 AM. (**d**) Representative images of MRGPRX4-expressing HEK293T

501   cells (shown by mCherry fluorescence) before and after application of 10 μM DCA. (**e**)

502   Representative traces of Ca^{2+} responses induced by application of 10 μM DCA, CA,

503   CDCA, or LCA. n = 50 cells each.

504   (**g-h**) MRGPRX4 is coupled to the Gq-PLC-Ca^{2+} signaling pathway. DCA (10 μM)

505   evoked a robust Ca^{2+} signal in MRGPRX4-expressing HEK293T cells (**g**, left); this

506   response was blocked by pretreating cells for 30 min with the PLC inhibitor U73122

507   (**g**, middle), but not the Gβγ inhibitor gallein (**g**, right). Triton X-100 was used as a

508   positive control. The summary data are shown in (**h**); n = 7-10 cells each. Student's

509   *t*-test, ***$p < 0.001$, and n.s. = not significant ($p > 0.05$).

510   (**i-k**) Identification of key residues in MRGPRX4 that mediate ligand binding and

511   receptor activation. (**i**) Primary sequence alignment of the human MRGPRX1,

512   MRGPRX2, MRGPRX3, and MRGPRX4 proteins. The positions of the three amino

513   acids in MRGPRX4 that were mutated to alanine are shown at the right. (**j**)

514   Dose-dependent activation of wild-type (WT) MRGPRX4 and three MRGPRX4

515   mutants with the indicated point mutations was measured using the TGFα shedding

516   assay. n = 1 experiment performed in triplicate. (**k**) Plasma membrane expression of

517   Myc-tagged WT and mutant MRGPRX4 was measured using an anti-Myc antibody

518   and normalized to WT MRGPRX4 expression.

519

520   **Fig. 4. A subset of human DRG neurons express MRGPRX4 and respond to bile**

521   **acids.**

522   (**a-d**) Representative DRG sections showing *in situ* hybridization (ISH, **a**) and

523   immunohistochemistry (IHC, **b**) for MRGPRX4; the summary data are shown in (**c**); n

524   = 2234 and 2735 neurons for ISH and IHC, respectively. The scale bars represent

525   200 μm (**a**) and 100 μm (**b**). (**d**) Diameter distribution for all 2234 DRG neurons

526 measured using *in situ* hybridization, 124 MRGPRX4-positive neurons, and 788

527 TrkA-positive neurons.

528 (**e**) Flow chart depicting the steps for characterizing the gene expression profiles of

529 human DRG samples using triple-color RNAscope *in situ* hybridization.

530 (**f**) Representative RNAscope images of *MRGPRX4* and other genes in human DRG

531 sections. Each fluorescent dot indicates a single mRNA transcript. Scale bar, 10 μm.

532 (**g**) Quantification of the gene expression data shown in (**f**). A neuron was defined as

533 positive if $\geq$ 20 fluorescent dots in the respective mRNA channel were detected in

534 that neuron.

535 (**h**) Bile acids induced a Ca^{2+} response in a subset of cultured human DRG neurons.

536 (**left**) Representative bright-field images and Fluo-8 fluorescence images of two

537 different DRG cultures from one embryo donor one adult donor. (**right**)

538 Representative traces of individual DCA-responsive DRG neurons (circled by the

539 dash line in (**left**)). Pseudo-color images of chemical-induced signals are shown

540 under each trace. C15 (compound 15), CA, DCA, and His (histamine): 100 μM each;

541 KCl: 75 mM. Veh, vehicle. Scale bar, 50 μm.

542 (**i**) Percentage of human DRG neurons that were responsive to the indicated tested

543 compounds measured as in (**h**).

544 (**j**) Venn diagram of the cultured human DRG neurons that were activated by the

545 indicated tested compounds. Green represents DCA responded neurons; Heavy gray

546 represents capsaicin responded neurons; light gray represents histamine responded

547 neurons.

548

Fig. 5 Bile acids and MRGPRX4 specific agonist induce histamine-independent itch in human.

(a1-a2) Itch evoked by a double-blind intradermal injection of DCA and nateglinide (Nat) in human subjects. (25 µl for each injection) (**a1**) Time course of the perceived itch intensity (n = 18-32). The traces are plotted with the standard error of the mean (s.e.m.) at the peak of each trace. The descriptions of the itch intensity are shown on the right. The injection sites on the subject's forearm are indicated. X4, MRGPRX4 (**a2**) Summary of the area-under-the-curve (AUC) of the itch intensity traces shown in (**a1**).

(b1-b2) Itch evoked by the indicated doses of DCA (25 µl for each injection, n = 8-14). The linear regression analysis of concentration versus the AUC is showed as a red line.

(c1-c2) Itch evoked by CDCA, CA, TCDCA, and LCA (25 µl for each injection, n = 10-31). The vehicle data (Veh) is reproduced from (**a1**).

(d1-d2) DCA-evoked itch is not inhibited by antihistamine (Anti-His). (**d1**) Time course of itch intensity evoked by an intradermal injection of DCA or histamine (His) following antihistamine or placebo pretreatment (25 µl for each injection, n = 12-14). Each pair of dots connected by a gray line represents an individual subject.

Student's *t*-test, **$p < 0.01$, ***$p < 0.001$, and n.s. = not significant ($p > 0.05$).

568

Fig. 6 TGR5 does not serve as an itch receptor in human

570   (**a1-a2**) Intradermal injection of a non-bile acid TGR5 agonist compound 15 (C15)

571   does not induce itch in human. (**a1**) Time course of the perceived intensity of itch

572   evoked by DCA and vehicle are reproduced from **Fig. 5a1**, and the itch evoked by

573   C15 is from 19 subjects. The equivalent concentration (equiv. conc.) of DCA and C15

574   means the fold of concentration to the EC_{50} of activating human TGR5. (**a2**) The

575   quantification results of area under curve (AUC) of itch intensity shown in (**a1**) (mean

576   ± s.e.m.). Veh, vehicle. Student's t-test, ***p < 0.001, and n.s. not significant (p >

577   0.05).

578   (**b-c**) The activation of human MRGPRX4 (**b**) or human TGR5 (**c**) by DCA (red),

579   compound 15 (C15, green) and nateglinide in MRGPRX4- or TGR5-expressing

580   HEK293T cells detected by FLIPR and luciferase assay respectively..

581   (**d**) The relationship between the evoked itch and the relative potency to activate

582   human MRGPRX4 or human TGR5 by the specific agonists of these two receptors.

583   The Y-axis shows the relative activation of certain compound to the receptor,

584   representing the logarithm of (maximal response/EC_{50}). The X-axis shows the

585   human itch intensity, representing the AUC of itch evoked by certain compound.

586   Statistic test was performed between the itch intensity of compound 15 and vehicle,

587   or between the itch intensity of nateglinide and vehicle. Nat, nateglinide; C15,

588   compound 15; Veh, vehicle. Student's t-test, **$p < 0.01$, and n.s. not significant ($p >$

589   0.05).

590   (**e**) *In situ* hybridization (ISH) of TGR5 in human DRG sections. (**left**) The diagram

591   depicting the morphology of DRG neurons and surrounding satellite glial cells.

592   (**middle and right**) TGR5 was highly expressed in satellite glial cells (indicated by

593   arrows) but not DRG neurons in human DRG. Scale bar, 50 µm

594   (**f**) *In situ* hybridization of TGR5 in mouse DRG sections. TGR5 was highly expressed

595   in DRG neurons (indicated by arrow heads) in mouse DRG. Scale bar, 50 µm

596   (**g-h**) Immunohistochemistry (IHC) of human and mouse DRG sections. (**g**) In human

597   DRG, TGR5 was expressed in satellite glial cells (indicated by arrows) but not in

598   neurons (marked by NeuN, indicated by arrow heads). (**h**) In mouse DRG, TGR5 was

599   expressed in neurons (marked by NeuN, indicated by arrow heads). Scale bar, 50 µ

600   m.

601   (**i**) Quantification of the percentage of TGR5+ neurons (over NeuN+ neurons) in

602   human and mouse DRG (immunohistochemistry). Chi-square test, **$p < 0.01$.

603

604   **Fig. 7 Elevated bile acids are correlated with the occurrence of itch among**

605   **patients with liver disease and are sufficient to activate MRGPRX4.**

606   (**a-b**) Summary of individual bile acid levels (**a**) and total bile acid levels (**b**, the sum of

607   the 12 bile acids shown in **a**) in itchy patients with liver diseases (Liver_itch, n = 27),

608   non-itchy patients liver diseases, (Liver_non-itch, n = 36), and itchy patients with

609   dermatic diseases (Skin_itch, n = 8). The plasma bile acid levels were measured

610   using HPLC-MS/MS (inset).

611   (**c-d**) Summary of individual bile acid levels (**c**) and total bile acid levels (**d**, the sum of

612   the 12 bile acids shown in **c**) in 13 patients with liver diseases during itch and after

613   itch relief. The inset shows the separation of standard bile acids by HPLC-MS/MS.

614 (**e-f**) Left, Ca^{2+} responses in MRGPRX4-expressing HEK293T cells induced by

615 application of a mixture of artificial bile acids derived from itchy patients with liver

616 diseases and healthy subjects. The Ca^{2+} signal was measured using Fluo-8 and was

617 normalized to the signal measured using the 1x liver_itch mix. The summary data are

618 shown in (**f**); n = 50 cells each.

619 (**g**) Proposed model depicting the mechanism underlying itch in patients with liver

620 diseases. In itchy patients, accumulated bile acids reach the skin via the circulatory

621 system, where they activate nerve fibers in a subset of MRGPRX4-expressing DRG

622 neurons. These activated neurons relay the itch signal to the spinal cord and higher

623 brain centers, eliciting the sensation of itch.

624 Student's *t*-test, *$p < 0.05$, **$p < 0.01$, ***$p < 0.001$.

625 **Supplementary figures**

626

627 **Supplementary Fig. 1 Construct design and surface expression of candidate**

628 **GPCRs in HEK293T cells.**

629 (**a**) Map of the generic GPCR expression vector. The 3′ and 5′ terminal repeats (TR)

630 are recognized by the PiggyBac transposase. Myc, Myc tag; $Puro^R$,

631 puromycin-resistance gene.

632 (**b**) Plasma membrane expression of the indicated GPCRs transiently expressed in

633 HEK293T cells, detected using an anti-Myc antibody. Scale bar, 20 μm.

634

635 **Supplementary Fig. 2 ^{1}H-NMR analysis of bile acids in fractions F1, F2, F3, F4,**

636 **and F6**

637 The hydrogen chemical shift of CA, CDCA, DCA, and LCA at carbon 3, 7, 12 were

638 determined by ^{1}H-NMR. Note that the active fractions (F2 through F4) contained the

639 characteristic hydrogen peaks corresponding to these bile acids.

640

641 **Supplementary Fig. 3 Human MRGPRX4, but not human MRGPRX1-3 or mouse**

642 **and rat Mrgpr family members, are activated by bile acids.**

643 (**a**) Phylogenetic analysis of mouse (Mm, green), rat (Rn, blue), rhesus monkey (Rh,

644 black), and human (Hs, red) Mas-related GPCR (mrg) family members. Amino acid

645 sequence similarity compared to Hs. MRGPRX4 is shown in the parenthesis.

646 (**b-f**) Activation of human MRGPRX1-4 by CA, CDCA, DCA, LCA and Nateglinide

647 (100 μM each, n = 100 cells from two experiments). Human MRGPRX1-4 were stably

648 expressed in HEK293T cells, and activation was measured using the Ca^{2+} indicator

649 Fluo-8. Responses are normalized to Bam8-22 (20 μM), PAMP9-20 (20 μM), ATP

650 (50 μM), and DCA (100 μM) for MRGPRX1, MRGPRX2, MRGPRX3, and

651 MRGPRX4, respectively. The data for MRGPRX4 (**e**) are reproduced from **Fig. 3f**.

652 (**g-h**) Mouse and rat Mrgpr family members are not activated by DCA (100 μM, n = 6

653 cells) or a mixture of DCA and LCA mix (20 μM each, n = 50 cells).

654

655 **Supplementary Fig. 4 The anti-MRGPRX4 antibody has high specificity.**

656   HEK293T cells were transiently transfected with MRGPRX1, MRGPRX2, MRGPRX3,

657   or MRGPRX4. The anti-MRGPRX4 antibody (Abcam, ab120808, 1:200 dilution)

658   specifically labeled MRGPRX4-expressing HEK293T cells, but not MRGPRX1-,

659   MRGPRX2-, or MRGPRX3-expressing cells. Transfected cells were identified by

660   mCherry fluorescence, and the nuclei were counterstained with DAPI. Scale bar, 50

661   μm.

662

663   **Supplementary Fig. 5 Expressing MRGPRX4 in cultured rat DRG neurons**

664   **renders the cells responsive to bile acids.**

665   (**a**)   Top,   cultured   rat   DRG   neurons   were   transfected   with   the

666   pPiggyBac-CAG-MRGPRX4-P2A-mCherry plasmid by electroporation. The cells

667   circled by dashed lines are an MRGPRX4-positive neuron (neuron 2 with red

668   fluorescence)   and   an   MRGPRX4-negative   (neuron   1)   neuron.   Bottom,

669   non-transfected cultured rat DRG neurons. A representative neuron (neuron 3) is

670   circled by a dash line. Scale bar, 50 μm.

671   (**b**) Representative traces from the cells indicated in (**a**). DCA and CA: 10 μM;

672   capsaicin (Cap): 1 μM; KCl: 75 mM.

673   (**c**) Summary of the amplitude and percentage of Ca^{2+} signals in response to DCA

674   and CA. Responsive neurons were defined as exceeding a threshold of 20% $\Delta F/F_0$.

675   n = 60-77 neurons per group.

676   (**d**) Summary of the amplitude and percentage of Ca^{2+} signals in response to

677   capsaicin and KCl. Responsive neurons were defined as in (**c**). n = 67-95 neurons per

678   group.

679   Student's *t*-test or two-proportion z-test, *$p < 0.05$, **$p < 0.01$, ***$p < 0.001$, and n.s. =

680   not significant ($p > 0.05$).

681

682   **Supplementary Fig. 6 Cultured human DRG neurons respond to various**

683   **chemicals.**

684   Ca^{2+} imaging of human DRG neurons from one human embryo (donor 1) and three

685   adult donors (donors 2-4).

686   (**a**) Representative bright-field and fluorescence images of cultured human DRG

687   neurons. Scale bar, 50 μm.

688   (**b**) Representative Ca^{2+} traces in response to the indicated test compounds

689   measured in the cells shown in (**a**). Veh, vehicle. Compound 15 (C15), CA and DCA:

690   100 μM; histamine (His): 50 μM; capsaicin (Cap): 1 μM; KCl: 75 mM.

691   (**c**) Summary of the percentage of neurons that responded to the indicated test

692   compounds (defined as exceeding a threshold of > 20% $\Delta F/F_0$).

693

694

695

696

697   **Supplementary Fig. 7 Expression of TGR5 in mouse and monkey DRG**

698　(**a**) Phylogenetic analysis of mouse (Mm.), rat (Rn.), rhesus monkey (Rh,) and human

699　(Hs,) TGR5. Amino acid sequence similarity compared to Hs. TGR5 is shown in the

700　parenthesis.

701　(**b**) The HEK293T cells were transiently transfected with human TGR5 expression

702　vector (pPiggyBac-TGR5-P2A-mCherry). The anti-TGR5 antibody can specifically

703　labeled the TGR5-expressing cells identified by the mCherry signal. The nuclei were

704　counterstained with DAPI. Arrow heads indicate the representative TGR5-expressing

705　cells. Scale bar, 20 μm.

706　(**c**) *In situ* hybridization (ISH) of TGR5 in mouse showing the morphology of mouse

707　DRG and the adjacent spinal cord. Scale bar, 100 μm.

708　(**d**) *In situ* hybridization of TGR5 in monkey (*Macaca mulatta*) DRG sections. TGR5

709　was highly expressed in satellite glial cells (indicated by arrows). Scale bar, 50 μm

710　(**e**) Immunohistochemistry (IHC) of monkey DRG sections. TGR5 was expressed in

711　satellite glial cells (indicated by arrows) but not neurons (marked by NeuN, indicated

712　by arrow heads). Scale bar, 50 μm.

713

714　**Supplementary Fig. 8 Quantification of bile acids in human plasma**

715　(**a**) Standard curve of 12 bile acids quantified by HPLC-MS/MS. All the 12 bile acids

716　show good linear correlation between the MS response and the concentration (0.1-1

717　μM)

718　(**b**) Quantification results of 8 bile acids shown in **Fig. 7a**.

719　(**c**) Quantification results of 8 bile acids shown in **Fig. 7c**.

720   All error bars represent the s.e.m.; student's t-test, *$p < 0.05$, and n.s. = not significant

721   ($p > 0.05$).

722

723   **Supplementary Fig 9. Bilirubin potentiates the activation of MRGPRX4 by bile**

724   **acids and may contribute to cholestatic itch.**

725   (**a**) Comparison of the activation of MRGPRX4 by DCA, bilirubin and taurine

726   conjugated bilirubin. Taurine conjugated bilirubin was used in order to mimic the

727   direct bilirubin under human physiological condition. MRGPRX4 was expressed in

728   HEK293T cells and the activation was measured by FLIPR assay.

729   (**b**) Bilirubin allosterically modulates the activation of MRGPRX4 by DCA. Different

730   concentrations of bilirubin was mixed with DCA, and then the activation of MRGPRX4

731   by these mixes was tested in MRGPRX4-expressing HEK293T cells using FLIPR

732   assay.

733   (**c**) DCA allosterically modulates the activation of MRGPRX4 by bilirubin, similar to

734   (**b**).

735   (**d**) Comparison of total bilirubin, direct bilirubin (conjugated) and indirect bilirubin

736   (unconjugated) level in liver disease patients with itch (Liver_itch) (n = 30) or without

737   itch (Liver_Non-itch) (n = 34), or patients with dermatic itch (Skin_itch) (n = 6).

738   (**e**) Comparison of total bilirubin, direct bilirubin and indirect bilirubin level in liver

739   disease patients (n=12) during itch and after itch relief.

740   (**f**) Correlation between itch intensity and plasma total bile acid, total bilirubin, direct

741   bilirubin, and indirect bilirubin. The itch intensity was directly reported by patients via a

742   questionnaire with 0 representing no itch and 10 the highest level of itch.

743   All error bars represent the s.e.m.. (**a-c**) One-way ANOVA, $*p < 0.05$, $**p < 0.01$, $***p$

744   < 0.001, and n.s. not significant ($p > 0.05$). (**d-f**) Student's t-test, $**p < 0.01$, $***p <$

745   0.001, and n.s. = not significant ($p > 0.05$).

746

747

748

749   **Supplementary Table. 1 Genes that are highly expressed in human DRG**

750

751   **Supplementary Table 2 GPCRs expression profiling in human DRG**

752   Red labeled genes are candidate GPCRs that are highly expressed in human DRG.

753   Blue labeled gene is TGR5.

754

755

756

757   **References**

758   1   Koch, S. C., Acton, D. & Goulding, M. Spinal Circuits for Touch, Pain, and Itch. *Annu Rev*

759   *Physiol* **80**, 189-217, doi:10.1146/annurev-physiol-022516-034303 (2018).

760   2   Tajiri, K. & Shimizu, Y. Recent advances in the management of pruritus in chronic liver

761   diseases. *World J Gastroenterol* **23**, 3418-3426, doi:10.3748/wjg.v23.i19.3418 (2017).

762   3   Thurmond, R. L., Gelfand, E. W. & Dunford, P. J. The role of histamine H1 and H4 receptors in

763 allergic inflammation: the search for new antihistamines. *Nat Rev Drug Discov* **7**, 41-53,

764 doi:10.1038/nrd2465 (2008).

765 4 Beuers, U., Kremer, A. E., Bolier, R. & Elferink, R. P. Pruritus in cholestasis: facts and fiction.

766 *Hepatology* **60**, 399-407, doi:10.1002/hep.26909 (2014).

767 5 Imam, M. H., Gossard, A. A., Sinakos, E. & Lindor, K. D. Pathogenesis and management of

768 pruritus in cholestatic liver disease. *J Gastroenterol Hepatol* **27**, 1150-1158,

769 doi:10.1111/j.1440-1746.2012.07109.x (2012).

770 6 Jenkins, J. K. & Boothby, L. A. Treatment of itching associated with intrahepatic cholestasis of

771 pregnancy. *Ann Pharmacother* **36**, 1462-1465, doi:10.1345/aph.1A479 (2002).

772 7 Kremer, A. E., Oude Elferink, R. P. J. & Beuers, U. Pathophysiology and current management

773 of pruritus in liver disease. *Clinics and Research in Hepatology and Gastroenterology* **35**,

774 89-97, doi:10.1016/j.clinre.2010.10.007 (2011).

775 8 Alemi, F. *et al.* The TGR5 receptor mediates bile acid-induced itch and analgesia. *J Clin Invest*

776 **123**, 1513-1530, doi:10.1172/JCI64551 (2013).

777 9 Lieu, T. *et al.* The bile acid receptor TGR5 activates the TRPA1 channel to induce itch in mice.

778 *Gastroenterology* **147**, 1417-1428, doi:10.1053/j.gastro.2014.08.042 (2014).

779 10 Cipriani, S. *et al.* Impaired Itching Perception in Murine Models of Cholestasis Is Supported by

780 Dysregulation of GPBAR1 Signaling. *PLoS One* **10**, e0129866,

781 doi:10.1371/journal.pone.0129866 (2015).

782 11 Meixiong, J. *et al.* Identification of a bilirubin receptor that may mediate a component of

783 cholestatic itch. *Elife* **8**, doi:10.7554/eLife.44116 (2019).

784 12 Belmonte, C. & Viana, F. Molecular and cellular limits to somatosensory specificity. *Mol Pain* **4**,

785   14, doi:10.1186/1744-8069-4-14 (2008).

786   13   Dong, X. & Dong, X. Peripheral and Central Mechanisms of Itch. *Neuron* **98**, 482-494,

787   doi:10.1016/j.neuron.2018.03.023 (2018).

788   14   Flegel, C., Manteniotis, S., Osthold, S., Hatt, H. & Gisselmann, G. Expression profile of ectopic

789   olfactory receptors determined by deep sequencing. *PLoS One* **8**, e55368 (2013).

790   15   Flegel, C. *et al.* RNA-seq analysis of human trigeminal and dorsal root ganglia with a focus on

791   chemoreceptors. *PLoS One* **10**, e0128951 (2015).

792   16   Liu, Q. *et al.* Sensory neuron-specific GPCR Mrgprs are itch receptors mediating

793   chloroquine-induced pruritus. *Cell* **139**, 1353-1365, doi:10.1016/j.cell.2009.11.034 (2009).

794   17   Liu, Q. *et al.* Mechanisms of itch evoked by beta-alanine. *J Neurosci* **32**, 14532-14537,

795   doi:10.1523/JNEUROSCI.3509-12.2012 (2012).

796   18   Hall, M. P. *et al.* Engineered luciferase reporter from a deep sea shrimp utilizing a novel

797   imidazopyrazinone substrate. *ACS Chem Biol* **7**, 1848-1857, doi:10.1021/cb3002478 (2012).

798   19   Inoue, A. *et al.* TGFalpha shedding assay: an accurate and versatile method for detecting

799   GPCR activation. *Nat Methods* **9**, 1021-1029, doi:10.1038/nmeth.2172 (2012).

800   20   Patapoutian, A. & Reichardt, L. F. Trk receptors: mediators of neurotrophin action. *Curr Opin*

801   *Neurobiol* **11**, 272-280 (2001).

802   21   Han, S. K., Mancino, V. & Simon, M. I. Phospholipase Cbeta 3 mediates the scratching

803   response activated by the histamine H1 receptor on C-fiber nociceptive neurons. *Neuron* **52**,

804   691-703, doi:10.1016/j.neuron.2006.09.036 (2006).

805   22   Imamachi, N. *et al.* TRPV1-expressing primary afferents generate behavioral responses to

806   pruritogens via multiple mechanisms. *PNAS* **106**, 11330 –11335 (2009).

807   23   Wilson, S. R. *et al.* TRPA1 is required for histamine-independent, Mas-related G

808   protein-coupled receptor-mediated itch. *Nat Neurosci* **14**, 595-602, doi:10.1038/nn.2789

809   (2011).

810   24   Usoskin, D. *et al.* Unbiased classification of sensory neuron types by large-scale single-cell

811   RNA sequencing. *Nat Neurosci* **18**, 145-153, doi:10.1038/nn.3881 (2015).

812   25   Li, C. L. *et al.* Somatosensory neuron types identified by high-coverage single-cell

813   RNA-sequencing and functional heterogeneity. *Cell Res* **26**, 83-102, doi:10.1038/cr.2015.149

814   (2016).

815   26   Green, B. G. *et al.* Evaluating the 'Labeled Magnitude Scale' for Measuring Sensations of

816   Taste and Smell. *Chemical Senses* **21**, 323–334 (1996).

817   27   Kroeze, W. K. *et al.* PRESTO-Tango as an open-source resource for interrogation of the

818   druggable human GPCRome. *Nat Struct Mol Biol* **22**, 362-369, doi:10.1038/nsmb.3014 (2015).

819   28   J. KIRBY, K. W. H., J. L. BURTON. Pruritic Effect of Bile Salts. *British Medical Journal* **4**,

820   693-695 (1974).

821   29   Varadi, D. P. Pruritus Induced by Crude Bile and Purified Bile Acids. *Arch Dermatol* **109**

822   (1974).

823   30   Hogenauer, K. *et al.* G-protein-coupled bile acid receptor 1 (GPBAR1, TGR5) agonists reduce

824   the production of proinflammatory cytokines and stabilize the alternative macrophage

825   phenotype. *J Med Chem* **57**, 10343-10354, doi:10.1021/jm501052c (2014).

826   31   Neale, G., Lewis, B., Weaver, V. & Panveliwalla, D. Serum bile acids in liver disease. *Gut* **12**,

827   145-152 (1971).

828   32   Freedman, M. R., Holzbach, R. T. & Ferguson, D. R. Pruritus in cholestasis no direct causative

829   role for bile acid retention. *The American Journal of Medicine* **70**, 1011-1016 (1981).

830   33   Bartholomew, T. C., Summerfield, J. A., Billing, B. H., Lawson, A. M. & Setchell, K. D. Bile acid

831   profiles of human serum and skin interstitial fluid and their relationship to pruritus studied by

832   gas chromatography-mass spectrometry. *Clin Sci (Lond)* **63**, 65-73 (1982).

833   34   Leslie Schoenfield & Sjovall, J. Bile acids on the skin of patients with pruritus hepatobiliary

834   disease. *Nature* **January 7**, 93-94 (1967).

835   35   Xiang, X. *et al.* High performance liquid chromatography-tandem mass spectrometry for the

836   determination of bile acid concentrations in human plasma. *J Chromatogr B Analyt Technol*

837   *Biomed Life Sci* **878**, 51-60, doi:10.1016/j.jchromb.2009.11.019 (2010).

838   36   Jenkins, H. H., Spencer, E. D., Weissgerber, A. J., Osborne, L. A. & Pellegrini, J. E.

839   Correlating an 11-point verbal numeric rating scale to a 4-point verbal rating scale in the

840   measurement of pruritus. *J Perianesth Nurs* **24**, 152-155, doi:10.1016/j.jopan.2009.01.010

841   (2009).

842   37   Lek, M. *et al.* Analysis of protein-coding genetic variation in 60,706 humans. *Nature* **536**,

843   285-291, doi:10.1038/nature19057 (2016).

844   38   Hill, R. NK1 (substance P) receptor antagonists--why are they not analgesic in humans?

845   *Trends Pharmacol Sci* **21**, 244-246 (2000).

846   39   Mogil, J. S. Animal models of pain: progress and challenges. *Nat Rev Neurosci* **10**, 283-294,

847   doi:10.1038/nrn2606 (2009).

848   40   Hug, A. & Weidner, N. From bench to beside to cure spinal cord injury: lost in translation? *Int*

849   *Rev Neurobiol* **106**, 173-196, doi:10.1016/B978-0-12-407178-0.00008-9 (2012).

850   41   Taneja, A., Di Iorio, V. L., Danhof, M. & Della Pasqua, O. Translation of drug effects from

851   experimental models of neuropathic pain and analgesia to humans. *Drug Discov Today* **17**,

852   837-849, doi:10.1016/j.drudis.2012.02.010 (2012).

853   42   Geenes, V. & Williamson, C. Intrahepatic cholestasis of pregnancy. *World J Gastroenterol* **15**,

854   2049-2066 (2009).

855   43   Yusa, K., Zhou, L., Li, M. A., Bradley, A. & Craig, N. L. A hyperactive piggyBac transposase for

856   mammalian   applications.   *Proc   Natl   Acad   Sci   U   S   A* **108**,   1531-1536,

857   doi:10.1073/pnas.1008322108 (2011).

858

859 **MATERIALS AND METHODS**

860 ***Analysis of GPCRs expressed in human DRG neurons***

861 The expression profile of all genes in hDRG neurons was compared to human

862 reference tissues, including trigeminal ganglia, brain, colon, liver, lung, muscle, and

863 testis[14,15]. To identify DRG-enriched GPCRs, we using the following formula: [(the

864 expression level of a given gene in the DRG)/(the total expression level of that gene

865 in all tissues)]; a value ≥0.5 was used to define DRG-enriched genes. The expression

866 level of a gene refers to the number of fragments per kilobase of exon per million

867 fragments mapped (FPKM) in the tissue transcriptome.

868

869 ***Bovine tissue extracts***

870 Fresh bovine heart, brain, kidney, spleen, and liver tissues (40 g each) were

871 dissected and then boiled for 5 min in 200 ml water. Acetic acid and HCl were then

872 added to a final concentration of 1 M and 20 mM, respectively, and the mixture was

873 homogenized thoroughly and then centrifuged at 11,000 rpm for 30 min. The

874 supernatant was collected and concentrated to a volume of 40 ml using a rotary

875 evaporator. Acetone (80 ml) was then added to the concentrated solution, and the

876 new solution was again centrifuged at 11,000 rpm for 30 minutes. The supernatant

877 was collected using a rotary evaporator and freeze-dried in a vacuum. The final

878 product was weighed, and equal amounts of each extract were used to test for

879 activity.

880

881 **_Generation of stable GPCR-expressing cell lines_**

882 Stable cell lines expressing orphan GPCRs were generated using the PiggyBac

883 Transposon System. In brief, each orphan GPCR was subcloned into the PiggyBac

884 Transposon vector and co-transfected with the hyperactive PiggyBac transposase[43]

885 into the HEK293T-based TGFα shedding reporter cell line[19] using polyethylenimine

886 (PEI). Receptor-expressing cells were selected and maintained in DMEM containing

887 10% fetal bovine serum (FBS), 1 µg/ml puromycin, 100 U penicillin, and 100 µg/ml

888 streptomycin in a humidified atmosphere at 37°C containing 5% CO_2.

889

890 **_TGFα shedding assay_**

891 Cultured cells expressing orphan GPCRs were rinsed once with Mg^{2+}-free and

892 Ca^{2+}-free phosphate-buffered saline (PBS) and then detached with 0.05% (w/v)

893 trypsin. The cell suspension was transferred to a 15-ml tube and centrifuged at 190x_g_

894 for 5 min. The supernatant was discarded, and the cell pellet was suspended in 10 ml

895 PBS and incubated for 15 min at room temperature (RT). The cells were

896 re-centrifuged and suspended in 4 ml HBSS (Hanks' balanced salt solution)

897 containing 5 mM HEPES (pH 7.4). The suspended cells were then seeded in a

898 96-well plate at 40,000-50,000 cells per well and placed in a 37ºC incubator in 5%

899 CO_2 for 30 min. A 10x stock solution of each drug was prepared in assay buffer

900 (HBSS containing 5 mM HEPES, pH 7.4), and 10 µl of 10x stock solution was added

901 to each well. The plate was then placed in the incubator for 2 hr, after which alkaline

902 phosphatase (AP) activity was measured in the conditioned media and cells.

903

FLIPR assay

905   HEK293T cells stably expressing human MRGPRX4 were seeded in 96-well plates at

906   a density of ~50,000 cells per well. The following day, the cells were loaded with

907   Fluo-8 (Screen Quest Fluo-8 No-Wash Calcium Assay Kit, AAT Bioquest, Cat. No.

908   36316) for 2 hr, and test compounds were added to the wells. The Fluo-8 signal was

909   measured using the FLIPR TETRA system (PerkinElmer).

910

Luciferase assay

912   We generated a luciferase reporter plasmid that encodes secreted NanoLuc under

913   the control of a cAMP response element (CRE) and a minimal promoter. The

914   hygromycin-resistance gene and EBFP driven by the SV40 promoter in the reporter

915   plasmid were used to generate stable cell lines. HEK293T cells were transfected with

916   this plasmid, and a stable cell line was generated by selecting with hygromycin.

917   This stable reporter cell line was then transfected with various GPCRs and used

918   to monitor the activation of these receptors. In brief, the cells were seeded in 96-well

919   plates; the next day, the culture medium was replaced, and compounds were added

920   to the wells; forskolin (10 μM final concentration) and 0.01% DMSO (v/v) were used

921   as positive and negative controls, respectively. The plates were incubated at 37°C in

922   5% CO_2 for 24 hr, after which a 10-μl aliquot of cell culture medium was removed from

923   each well and combined with 40 μl culture medium plus 50 μl assay buffer (containing

924   20 μM of the luciferase substrate coelenterazine); after 5 min incubation,

925 luminescence was measured using an EnVision plate reader (PerkinElmer).

926

927 ***Fractionation of bile acid components***

928 A commercially available bovine bile acid powder (126.6 mg) was loaded in a silica

929 gel column (DCM:MeOH = 10:1). The smaller fractions were combined to form six

930 larger fractions (F1 through F6) based on analytical thin-layer chromatography

931 performed using 0.25-mm silica gel 60-F plates. Flash chromatography was

932 performed using 200–400 mesh silica gel.

933

934 ***MS and NMR***

935 High-resolution mass spectrometry was performed at the Peking University Mass

936 Spectrometry Laboratory using a Bruker Fourier Transform Ion Cyclotron Resonance

937 Mass Spectrometer Solarix XR. ^{1}H-NMR spectra were recorded on a Bruker

938 400-MHz spectrometer at ambient temperature with $CDCl_3$ as the solvent.

939

940 **Immunostaining and flow cytometry analysis**

941 Suspended live HEK 293 cells stably expressing the point-mutated MRGPRX4 were

942 washed in washing buffer (1X PBS solution, mixed with 5% fatal bovine serum (FBS))

943 for 3 times. Then cells were incubated with primary antibody (Sigmal-Aldrich Cat. No.

944 C3956, 1:25 dilution) for 30 minutes, and secondary antibody (AAT Bioquest iFluro[TM]

945 Alexa 488 goat antirabbit IgG Cat. No. 1060423, 1:50 dilution) for 1 hour. Cells were

946 washed for two times after each antibody treatment. Next, cells were resuspended

947 with 300 uL to 500 uL FACS buffer, and fluorescence-activated cell-sorting analysis

948 was performed, using the BD FACS Calibor Flow cytometer (BD Biosciences), and

949 the data were analyzed using FlowJo software (Ver. 7.6.1).

950

951 ***Cultured human DRG neurons***

952 Collection of DRG tissue from adult humans was approved by the Committee for

953 Medical Science Research Ethics, Peking University Third Hospital

954 (IRB00006761-2015238), and collection from human embryos was approved by the

955 Reproductive Study Ethics Committee of Peking University Third Hospital

956 (2012SZ-013 and 2017SZ-043) and Beijing Anzhen Hospital (2014012x). DRG

957 tissues were obtained from adult patients undergoing surgical excision of a

958 schwannoma; the tissues were placed immediately in ice-cold DMEM/F12 medium.

959 The tissues were then cut into pieces <1 mm in size and treated with an enzyme

960 solution containing 5 mg/ml dispase and 1 mg/ml collagenase at 37°C for 1 hr. After

961 trituration and centrifugation, the cells were washed in 15% (w/v) bovine serum

962 albumin (BSA) resuspended in DMEM/F12 containing 10% FBS, plated on glass

963 coverslips coated with poly-D-lysine and laminin, cultured in an incubator at 37°C,

964 and used within 24 hr of plating.

965

966 ***Culture and electroporation of rodent DRG neurons***

967 Rat DRG tissues were obtained from the thoracic and lumbar vertebrae and placed in

968 ice-cold DMEM/F12 medium. The tissues were cut into pieces <1 mm in size and

969   then treated with an enzyme solution containing 5 mg/ml dispase and 1 mg/ml

970   collagenase at 37°C for 1 hr. After trituration and centrifugation, the cells were

971   washed in 15% BSA, resuspended in DMEM/F12 containing 10% FBS, plated on

972   glass coverslips coated with poly-D-lysine and laminin, cultured in an incubator at

973   37°C, and used within 24 hr of plating.

974   Rat DRG neurons were electroporated as follows. After washing the neurons with

975   15% BSA, the neurons were resuspended in DMEM/F12 and electroporated using a

976   P3 Primary Cell 4D-Nucleofector X Kit L (cat. no. V4XP-3012, Lonza) in accordance

977   with the manufacturer's instructions. After electroporation, the neurons were cultured

978   for 72 hr before use in order to allow the transgenes to express.

979

980   ***Ca^{2+} imaging***

981   For Ca^{2+} imaging experiments, cells were loaded at 37°C for 1 hr with 10 µg/ml Fluo-8

982   AM (AAT Bioquest, Inc.) supplemented with 0.01% Pluronic F-127 (w/v; Invitrogen).

983   Bile acids, bio-mimicked bile acid mixes, and/or various drugs to be tested were

984   added to the cells in a chamber containing a custom-made 8-channel perfusion valve

985   control system. Fluorescence images were acquired using a Nikon A1 confocal

986   microscope.

987

988   ***In situ hybridization and immunostaining***

989   Single colorimetric *in situ* hybridization in hDRG sections was performed as follows.

990   The sections were fixed in freshly prepared 4% paraformaldehyde (PFA) in PBS for

991   20 min at RT, and then washed in fresh-DEPC PBS (1:1000 DEPC was added to 1x

992   PBS immediately before use) and DEPC-pretreated PBS (1:1000 DEPC in PBS

993   overnight, followed by autoclaving) for 10 min each. The sections were then

994   immersed in a DEPC-containing antigen-retrieval solution containing 10 mM citric

995   acid, 0.05% Tween-20 (pH 6.0) in a 95°C water bath for 20 min, and then cooled at

996   RT for 30 min. After washing in DEPC-pretreated PBS for 10 min, the sections were

997   incubated in a Proteinase K solution (25 µg/mL in DEPC-pretreated water) for 20 min

998   and then washed in fresh-DEPC PBS and DEPC-pretreated PBS (10 min each). The

999   sections were incubated in freshly prepared acetylation solution containing 0.1 M TEA

1000   and 0.25% acetic anhydride in DEPC-pretreated water for 10 min at RT, followed by a

1001   10-min wash in DEPC-pretreated PBS. The prehybridization step was performed in

1002   probe-free hybridization buffer consisting of 50% formamide, 5x SSC, 0.3 mg/ml

1003   yeast tRNA, 100 µg/ml heparin, 1x Denhardt's solution, 0.1% Tween-20, 0.1%

1004   CHAPS, and 5 mM EDTA in RNase-free water at 62°C for 30 min in a humidified

1005   chamber, followed by an overnight hybridization step in hybridization buffer containing

1006   5 ng/µl DIG-labeled riboprobes at 62°C in a humidified chamber (under a Parafilm

1007   coverslip). After the hybridization step, the sections were washed in 0.2x SSC at 68°C

1008   (once for 15 min and twice for 30 min each), followed by blocking in PBS containing

1009   0.1% Triton X-100 and 20% horse serum for 1 hr at RT. The sections were then

1010   stained overnight at 4°C with pre-absorbed AP-conjugated sheep anti-DIG antibody

1011   (1:1000, Roche, cat. 11093274910) in PBS containing 0.1% Triton X-100 and 20%

1012   horse serum. The sections were washed 3 times for 10 min each in PBS containing

1013 0.1% Triton X-100, followed by overnight incubation in the dark in AP buffer

1014 containing 100 mM Tris (pH 9.5), 50 mM MgCl$_2$, 100 mM NaCl, 0.1% Tween-20, 5

1015 mM levamisole, 0.34 mg/ml NBT (Roche cat. no. 11383213001), and 0.17 mg/ml

1016 BCIP (Roche, cat. no. 1138221001) to allow the color reaction to develop. The

1017 sections were washed 3 times for 10 min each in PBS, and then fixed for 30 min in 4%

1018 PFA in PBS. The sections were quickly rinsed 5 times in ddH$_2$O, dried at 37°C for 1 hr,

1019 and dehydrated in xylene (3 times for 2 min each). Finally, the sections were mounted

1020 under a glass coverslip using Permount (Fisher).

1021 Immunostaining was performed using a rabbit anti-hMRGPRX4 antibody

1022 obtained (Abcam, cat. no. ab120808). The sections were fixed in freshly prepared 4%

1023 PFA in PBS for 20 min at RT and then washed in PBS containing 0.1% Triton X-100 3

1024 times for 10 min each, followed by block in PBS containing 0.1% Triton X-100 and 20%

1025 horse serum for 1 hour at RT. The sections were then incubated overnight in primary

1026 antibody at 4°C, washed with PBS containing 0.1% Triton X-100 3 times for 15 min

1027 each, and incubated with secondary antibody for 1 hour at RT. After washing with

1028 PBS 3 times for 15 min each, the sections were mounted under glass coverslips and

1029 Fluoromount-G (Invitrogen).

1030

1031 **RNAscope in situ hybridization**

1032 RNAscope *in situ* hybridization was performed in accordance with the manufacturer's

1033 instructions (Advanced Cell Diagnostics). In brief, human DRG sections were fixed,

1034 dehydrated, and treated with protease. The sections were then hybridized with the

1035 respective target probe for 2 hours at 40°C, followed by four-round signal

1036 amplification. The sections were then mounted under coverslips, sealed with nail

1037 polish, and stored in the dark at 4°C until imaged.

1038

1039 ***Human itch test***

1040 The human itch test studies were approved by the Committee for Protecting Human

1041 and Animal Subjects at the Department of Psychology, Peking University

1042 (#2018-05-02). Volunteers were students and faculty members recruited from Peking

1043 University. All subjects provided written informed consent and were provided with the

1044 experimental protocol. All injections were performed using an INJEX 30 needle-free

1045 injection system (INJEX Pharma GmbH, Berlin, Germany). We performed two studies

1046 as described below.

1047 In the first study (to measure bile acid□induced itch sensation), each tested

1048 compound was dissolved in physiological saline containing 7% Tween-80

1049 (Sigma-Aldrich). The injection sites were cleaned with rubbing alcohol, and 25 µl of

1050 each solution was injected intradermally on the volar surface of each arm. The same

1051 volume of vehicle (saline containing 7% Tween-80) served as the negative control.

1052 Itch was defined as the desire to initiate scratching during the experiment, and the

1053 subjects rate the perceived intensity according the generalized labeled magnitude

1054 scale (LMS) described by Green et al.[26]

1055 In the second study (to measure the effect of antihistamines on DCA-induced

1056 itch), two experimental sessions were performed, separated by 2 weeks, with 14 and

1057   12 subjects participating in the first and second sessions, respectively. Approximately

1058   1.5 g of topical antihistamine cream (doxepin hydrochloride cream, Chongqing

1059   Huapont Pharm. Co., China) or a placebo cream (cold cream, Eau Thermale Avène,

1060   Paris, France) was applied 2.5 hr before injection of DCA or histamine

1061   (Sigma-Aldrich); any unabsorbed cream was removed with alcohol. A 500 µg/25 µl

1062   solution of DCA was prepared as described above, and a 2.5 µg/25 µl solution of

1063   histamine was dissolved in saline; 25 µl of the DCA or histamine solution was injected

1064   into the volar surface of the arm as described above. In the first session, each subject

1065   received two intradermal injections of DCA (one at the antihistamine-treated site and

1066   one at the placebo-treated site). In the second session, each subject received two

1067   intradermal injections of histamine (one at the antihistamine-treated site and one at

1068   the placebo-treated site). The subjects then rate the itch sensation as described

1069   above.

1070

1071   ***Quantification of plasma bile acids and bilirubin***

1072   These experiments were approved by the Committee for Biomedical Ethics, Peking

1073   University First Hospital (2017-R-94). Itch intensity was measured using a self-report

1074   numerical rating scale (NRS)[36], and whole blood samples were collected from

1075   patients with skin diseases and patients with liver diseases. Plasma was obtained by

1076   centrifuging 2 ml of whole blood at 4°C, 11,000 g for 10 min; 100 µl of each plasma

1077   sample was then mixed with 400 µl acetonitrile and left to sit at 4°C for 20 min. The

1078   mixture was centrifuged, and the supernatant was dried in a rotatory evaporator

1079 (45°C under vacuum), and the dried residue was retrieved and dissolved in 60%

1080 methanol for further analysis.

1081 The bile acid level in plasma samples was measured using HPLC-MS/MS

1082 (Agilent model LC1260 QQQ 6495). Chromatographic separation was performed in

1083 an ACQUITY UPLC HSS T3 column (2.1 mm × 100 mm, 1.8 μm; Waters Corp.). The

1084 mobile phase consisted of solution A (water) and solution B (acetonitrile). The total

1085 running time was 23 min, and a linear gradient (0.3 ml/min) was applied as follows:

1086 0-2 min: 10% B - 40% B; 2-18 min: 40% B - 50% B; 18-19 min: 50-100% B; 19-20 min:

1087 100% B; 20-21 min: 100-10% B; 21-23 min: 10% B. The injection volume was 5 μl,

1088 and the mobile phase flow rate was 3 ml/min. Deoxycholic-2,2,4,4,11,11-d6 acid

1089 (Sigma, cat. no. 809675) was used as an internal standard.

1090 Total bilirubin and direct bilirubin values were obtained from the patients' hospital

1091 blood chemistry reports.

1092

1093 ***Statistical analysis***

1094 Summary data are presented as the mean ± SEM. Human subjects were randomly

1095 assigned to control and experimental groups, and the subjects and investigators were

1096 double-blinded with respect to the experiment treatments. Data were analyzed using

1097 the Student's *t*-test, two-proportion z-test, Chi-square test or One-way ANOVA and

1098 differences with a *P*-value of < 0.05 were considered significant.

1099

1100

Fig. 1 Identification of MRGPRX4 activated by bile extract.

Fig. 2 Identification of active components that activate MRGPRX4 from bile extract.
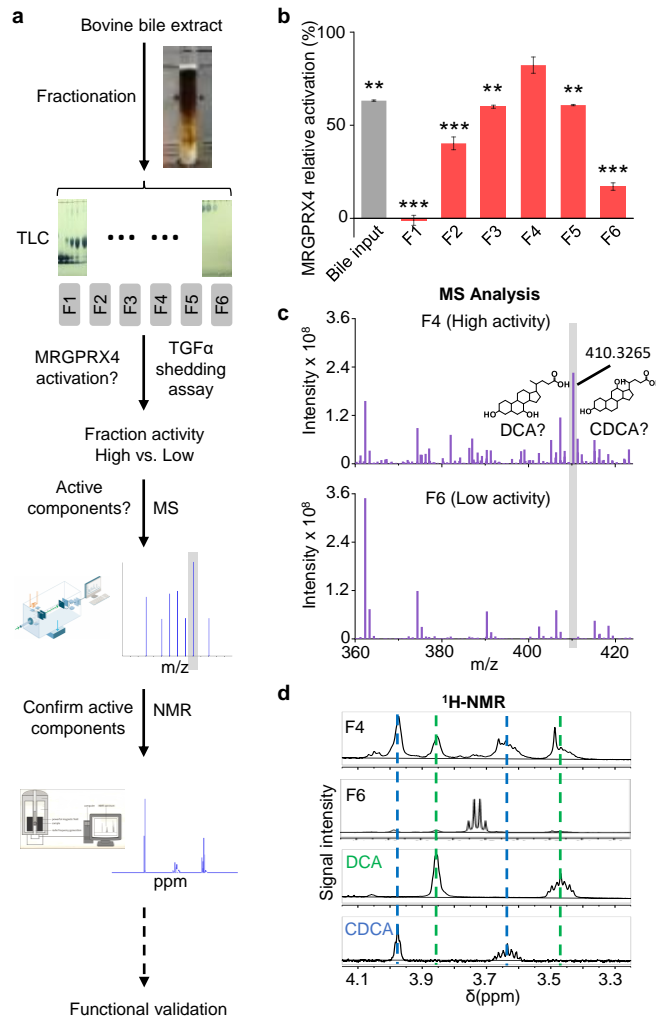
Fig. 3 Functional characterization and molecular profiling of bile acids as ligands for MRGPRX4
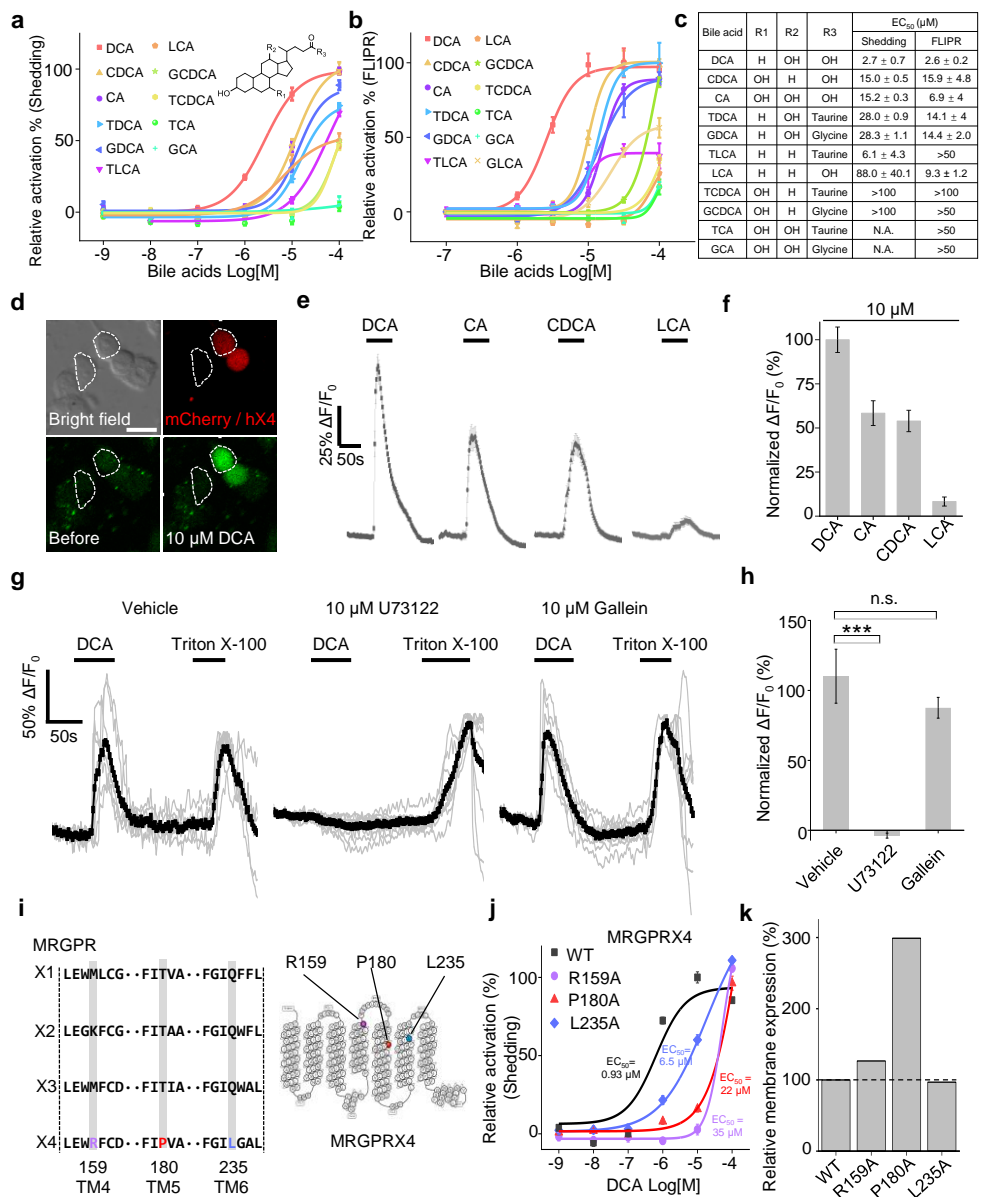
Fig. 4 A subset of hDRG neurons express MRGPRX4 and respond to bile acids.
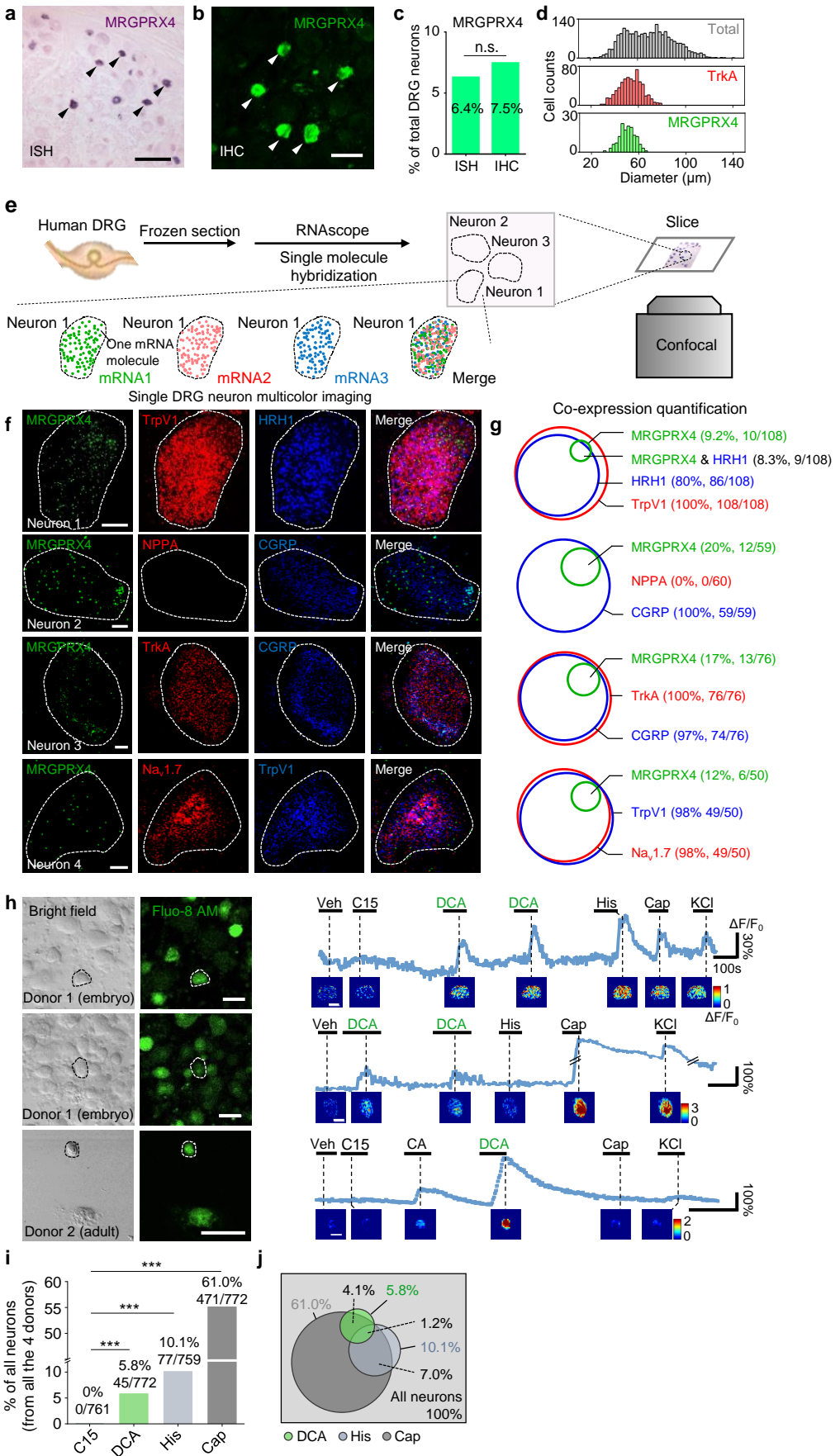
Fig. 5 Bile acids and MRGPRX4 specific agonist induce histamine-independent itch in human
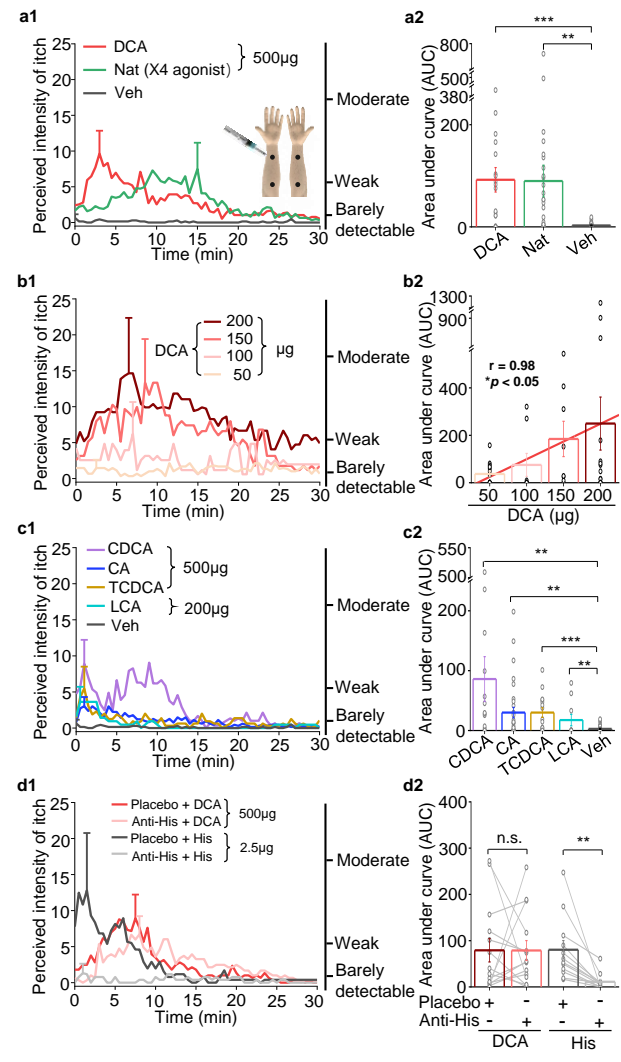
Fig. 6 TGR5 does not serve as an itch receptor in human
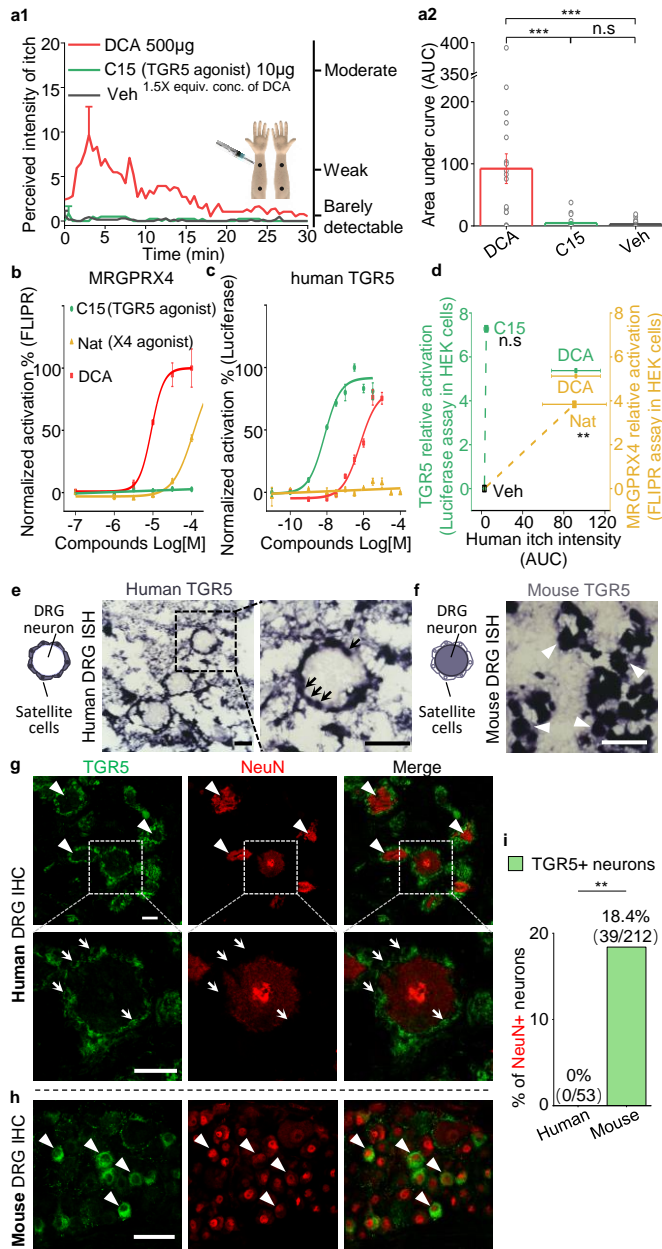
Fig. 7 Elevated bile acids correlate with the occurrence of itch among liver disease patients and are sufficient to activate MRGPRX4
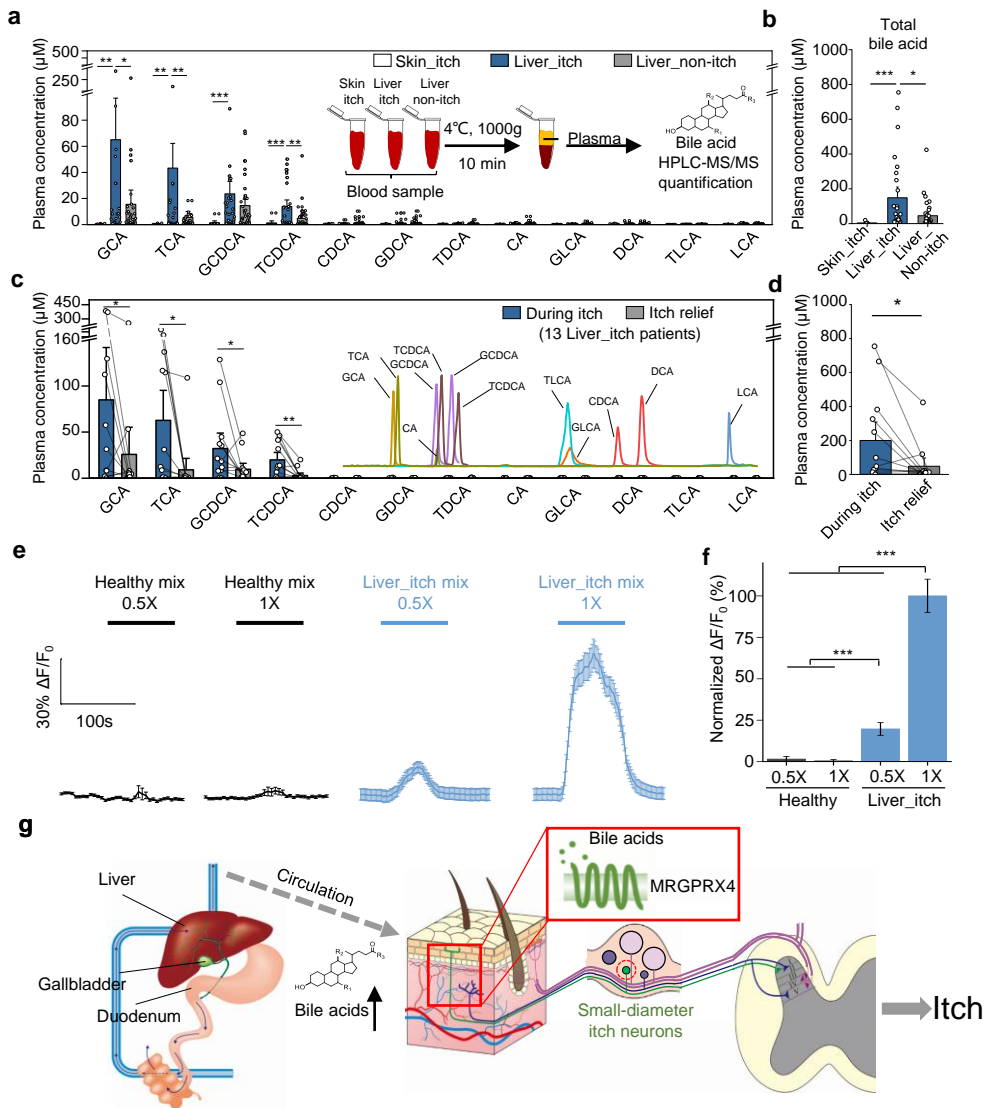
**Supplementary Fig. 1 Construct design and surface expression of candidate
GPCRs in HEK293T cells**
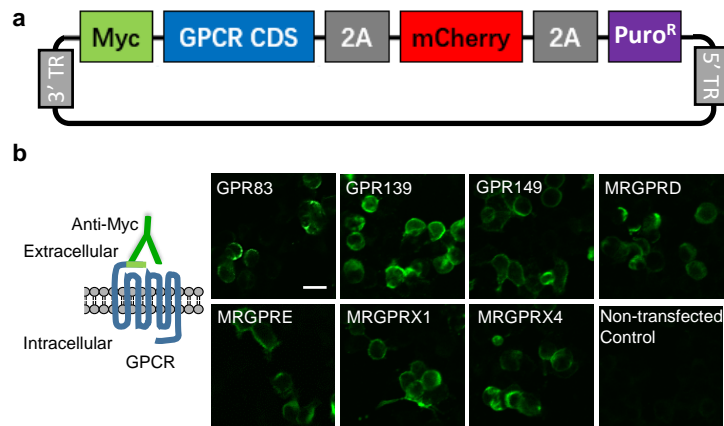
Supplementary Fig. 2 ¹H‑NMR analysis of bile acids in fractions F1, F2, F3, F4, and F6
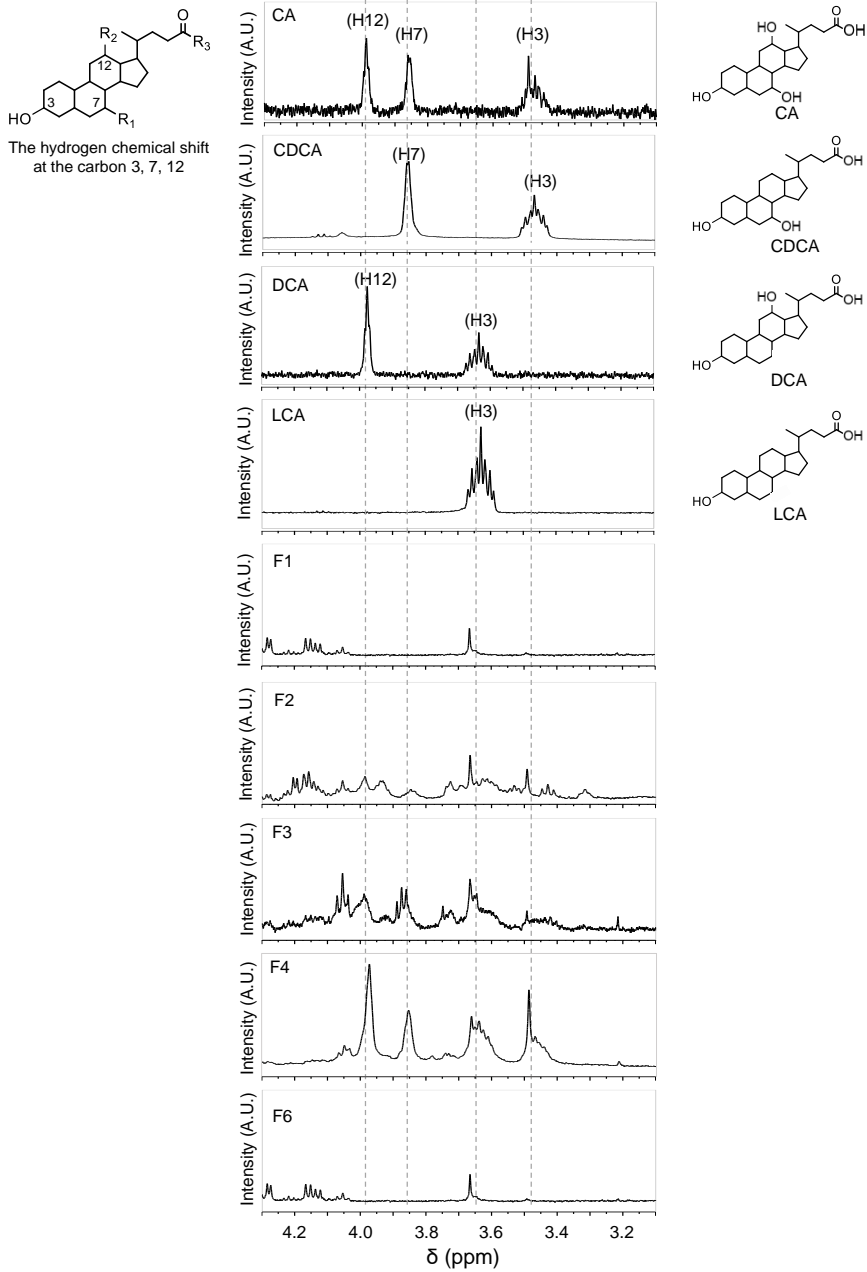
Supplementary Fig. 3 Human MRGPRX4, but not human MRGPRX1-3 or mouse and rat Mrgpr family members, are activated by bile acids.
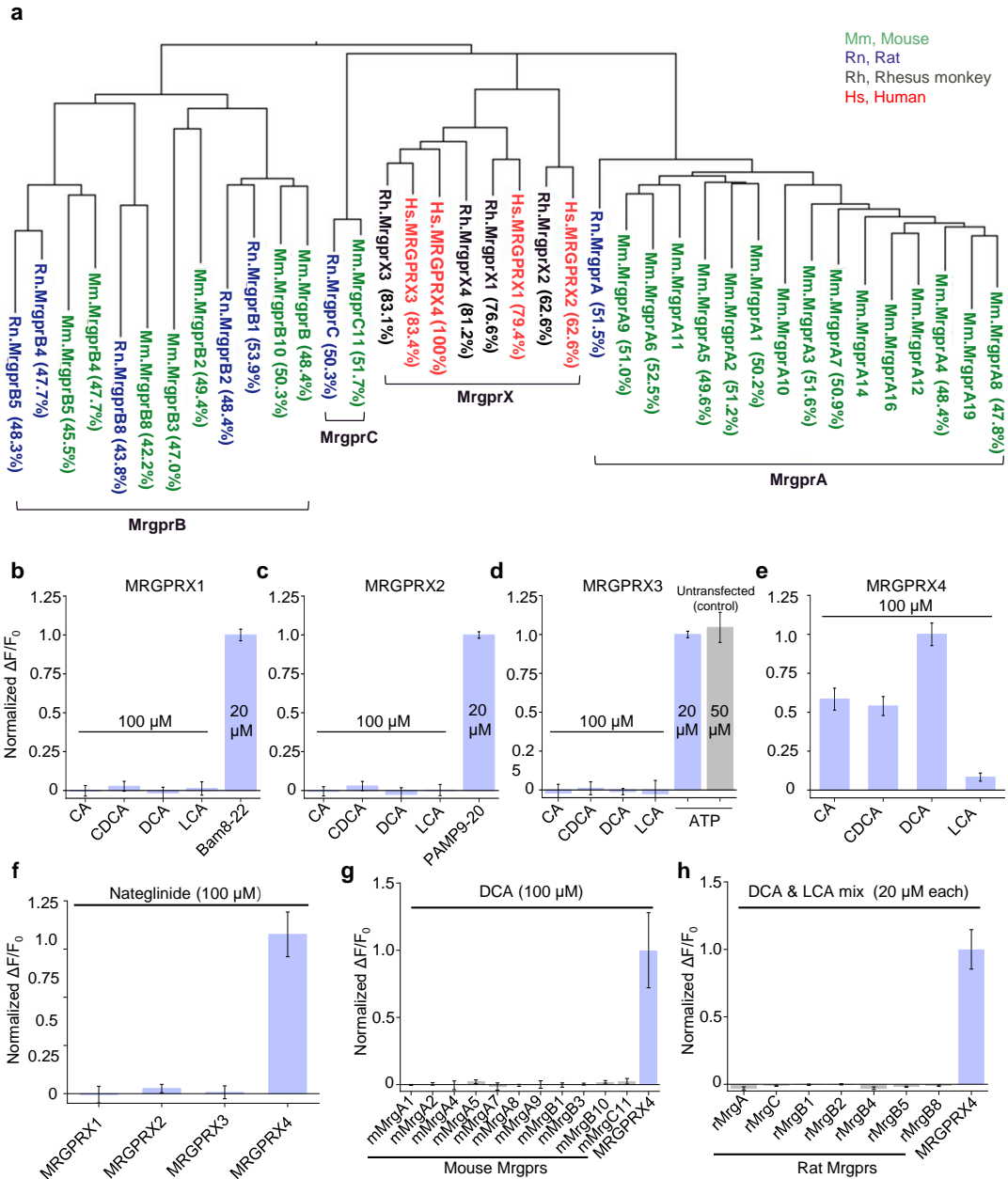
Supplementary Fig. 4 The anti-MRGPRX4 antibody has high specificity.
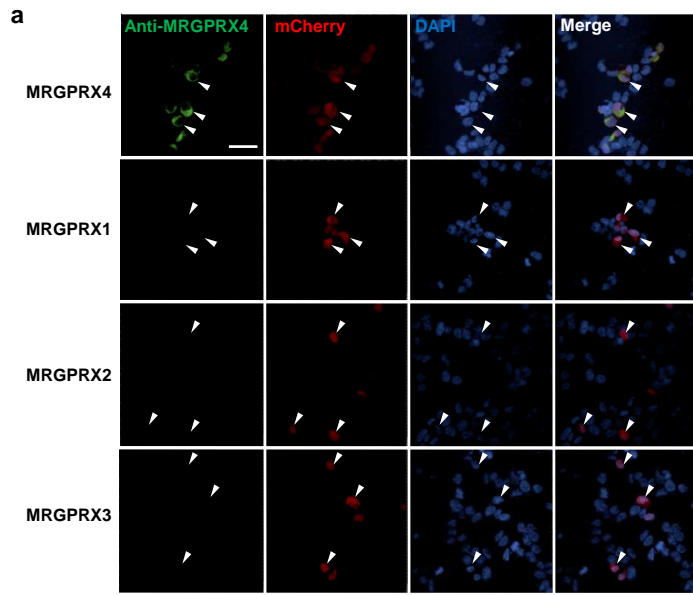
Supplementary Fig. S5. Expressing MRGPRX4 in cultured rat DRG neurons renders the cells responsive to bile acids.
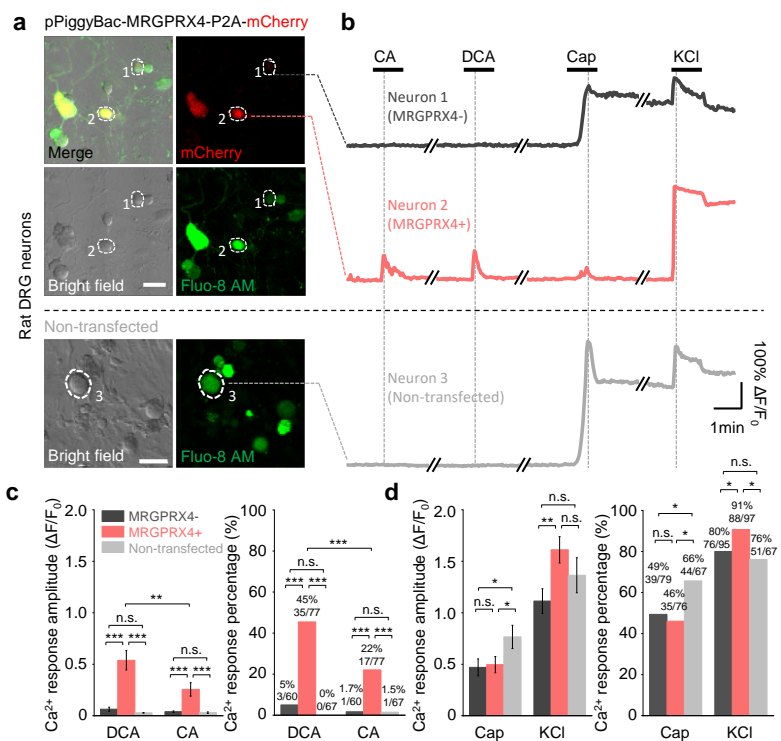
Supplementary Fig. 6 Cultured human DRG neurons respond to various chemicals
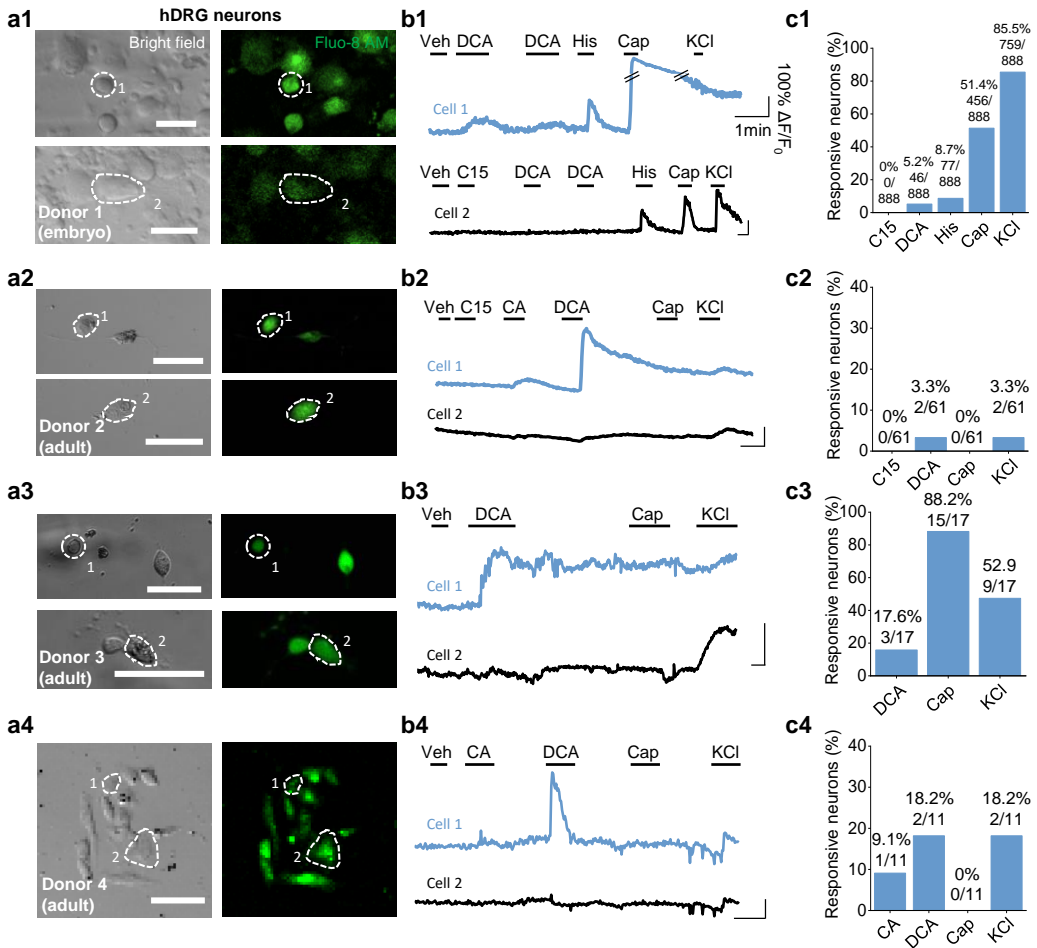
Supplementary Fig. 7 Expression of TGR5 in mouse and monkey DRG
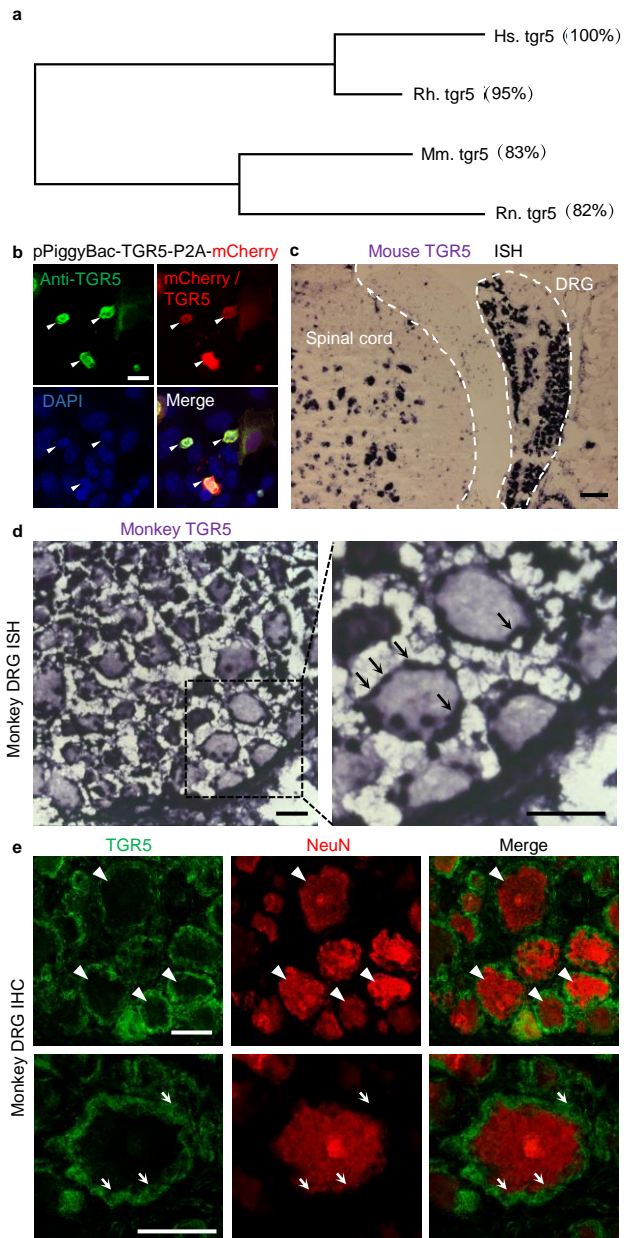
Supplementary Fig. 8 Quantification of bile acids in human plasma

Supplementary Fig. 9 Bilirubin is an allosteric modulator and potentiates the activation of MRGPRX4 by bile acids and may contribute to cholestatic itch

Supplementary Table 1 Genes that are highly expressed in human DRG

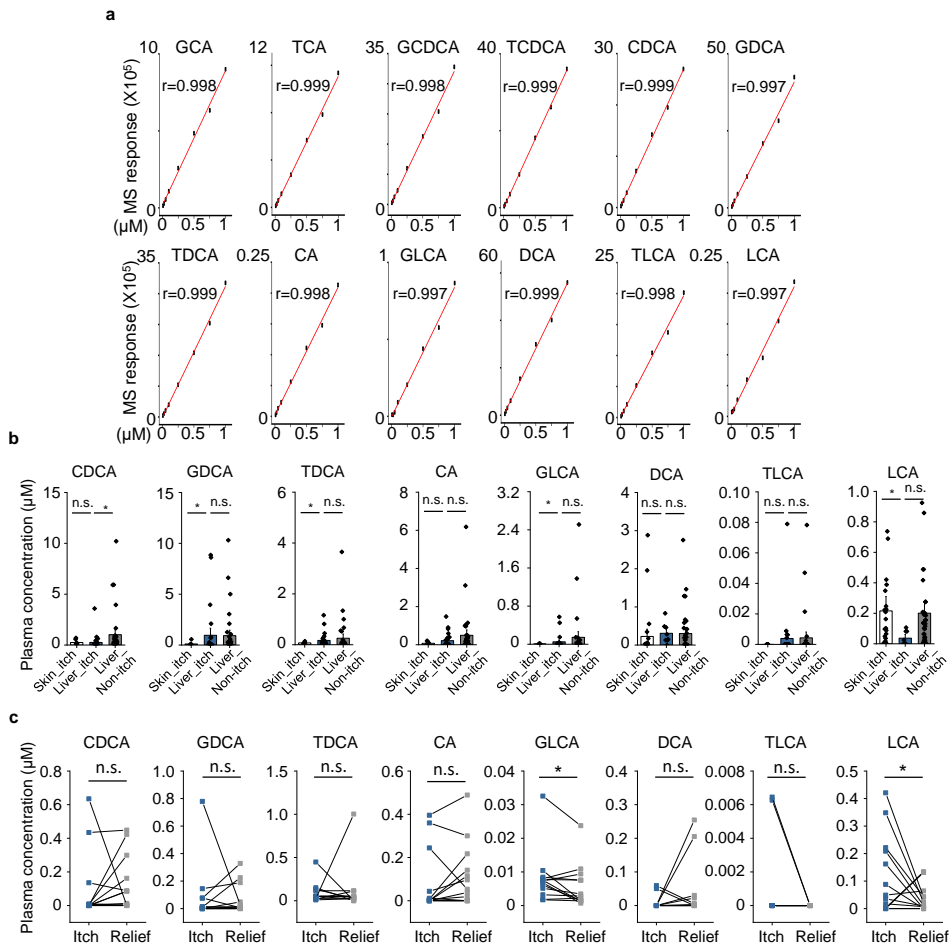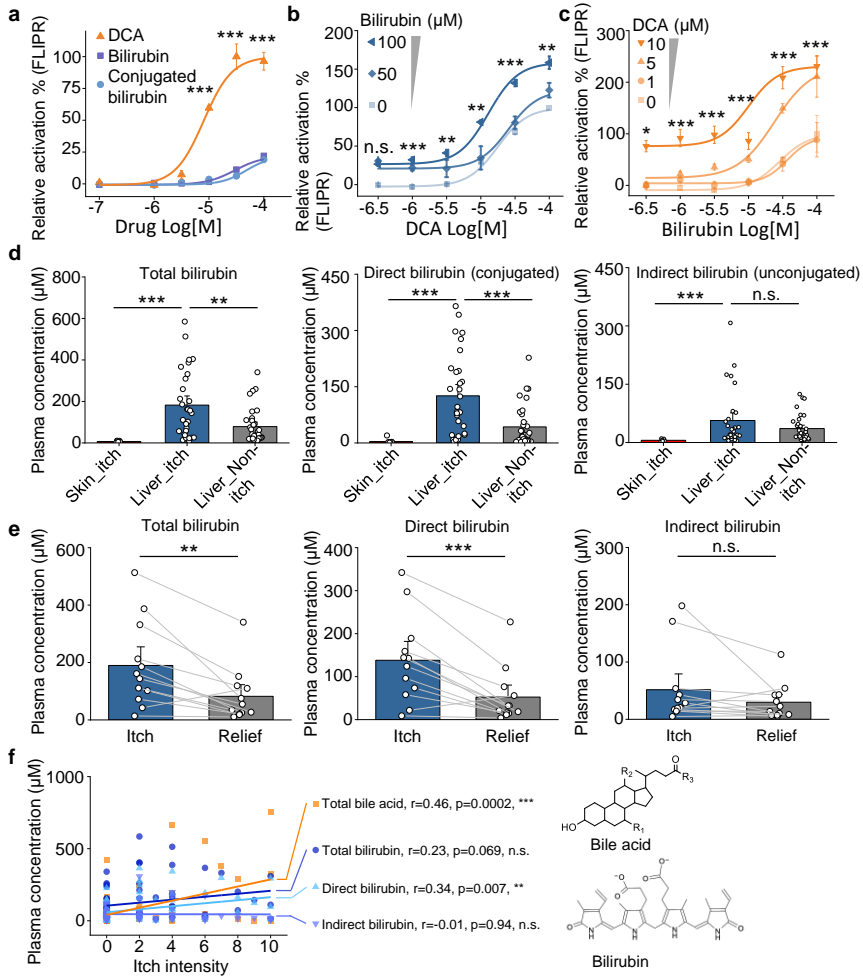| Rank	gene	DRG/All	Rank	gene	DRG/All	Rank	gene	DRG/All	Rank	gene	DRG/All	Rank	gene	DRG/All
1	LOC401164	1.0000	68	CCDC140	0.6985	135	ANKRD33	0.6209	202	GGT8P	0.5634	269	MAP7D2	0.5279
2	LOC645591	1.0000	69	PIRT	0.6964	136	CHRNA6	0.6181	203	CHRM4	0.5629	270	LOC100289511	0.5278
3	MIR1250	1.0000	70	VAT1L	0.6962	137	EPN3	0.6181	204	HOXC6	0.5627	271	SLC10A2	0.5276
4	MIR1914	1.0000	71	KRT75	0.6956	138	LIPM	0.6166	205	LOC100130298	0.5623	272	HSPA12A	0.5275
5	MIR3188	1.0000	72	HHLA1	0.6948	139	NBPF11	0.6150	206	LPAR3	0.5623	273	CYP4F24P	0.5273
6	MIR572	1.0000	73	RET	0.6899	140	KANK4	0.6145	207	FLJ42969	0.5611	274	RPL21P28	0.5260
7	MIR659	1.0000	74	GSX1	0.6867	141	OR13C5	0.6145	208	SLC2A6	0.5609	275	B4GALNT1	0.5253
8	MIR92B	1.0000	75	SCN10A	0.6867	142	SPDYE2	0.6136	209	FGF22	0.5606	276	CD1A	0.5253
9	MSGN1	1.0000	76	INSC	0.6863	143	PCDHAC2	0.6122	210	GRM4	0.5602	277	AATK	0.5249
10	OR10A4	1.0000	77	KCNK18	0.6858	144	PLD4	0.6120	211	FOXD3	0.5600	278	RXRG	0.5249
11	OR2M4	1.0000	78	OR2L13	0.6853	145	LOC100329108	0.6109	212	NKAIN4	0.5598	279	CRYBA2	0.5228
12	OR4H6P	1.0000	79	PRPH	0.6849	146	TRPV1	0.6099	213	LCNL1	0.5590	280	KCNA10	0.5221
13	OR56B2P	1.0000	80	LOC441617	0.6846	147	HOXD1	0.6098	214	TLX2	0.5588	281	SYT2	0.5214
14	P2RX6P	1.0000	81	SPTBN5	0.6845	148	OR56B4	0.6094	215	LOC100130275	0.5585	282	TSPAN10	0.5208
15	OR4N5	0.9985	82	SNORD123	0.6834	149	TLX3	0.6086	216	PDE6H	0.5579	283	SNORD116-21	0.5202
16	OR13C9	0.9799	83	CALCB	0.6819	150	PROKR2	0.6083	217	FOXS1	0.5576	284	INSRR	0.5201
17	SNORD87	0.9791	84	TMEM72	0.6789	151	KCNG4	0.6077	218	CHST8	0.5574	285	TUBB2A	0.5200
18	MIR324	0.9375	85	ADAMTS16	0.6761	152	NPSR1	0.6069	219	F2RL2	0.5564	286	C18orf42	0.5200
19	DYTN	0.9317	86	SNORA70B	0.6760	153	EGFL8	0.6065	220	MIR1247	0.5559	287	RESP18	0.5187
20	CRYGB	0.9233	87	MIR630	0.6754	154	FZD2	0.6061	221	GPR149	0.5547	288	PCDHAC1	0.5187
21	OR2M3	0.8983	88	SYT6	0.6753	155	SNORD125	0.6054	222	EMILIN3	0.5540	289	FLJ42875	0.5182
22	GPR139	0.8873	89	OR2T33	0.6725	156	TSHB	0.6045	223	TMEFF2	0.5527	290	OR2T32P	0.5177
23	MRGPRX4	0.8862	90	OTOP3	0.6707	157	KRT14	0.6042	224	HOXC4	0.5515	291	FCRLB	0.5170
24	SNORD91A	0.8861	91	BMP8B	0.6673	158	RASA4	0.6040	225	SLC3A1	0.5515	292	TMEM183B	0.5169
25	NOTO	0.8811	92	ISL2	0.6670	159	GLRA4	0.6034	226	MMD2	0.5508	293	THY1	0.5155
26	KRT32	0.8781	93	ENTPD2	0.6663	160	CHAT	0.6033	227	COL28A1	0.5498	294	FGF13	0.5154
27	NCRNA00052	0.8666	94	LOC644145	0.6660	161	C13orf36	0.6030	228	OR2W3	0.5496	295	LOC646329	0.5141
28	OR7E89P	0.8631	95	FAM19A3	0.6643	162	TTTY22	0.6019	229	PCSK2	0.5490	296	LOC100129726	0.5140
29	HCRT	0.8601	96	OR2T12	0.6639	163	POLR3G	0.6010	230	MIXL1	0.5477	297	SLITRK2	0.5140
30	MIR3907	0.8565	97	FGFBP3	0.6628	164	TTC24	0.6004	231	CADM3	0.5461	298	SHISA3	0.5138
31	OR2M1P	0.8519	98	TUSC5	0.6624	165	PRX	0.5978	232	BEAN1	0.5456	299	TMC3	0.5132
32	MRGPRX1	0.8291	99	CHRNA9	0.6583	166	LOC285401	0.5971	233	LOC645431	0.5454	300	P2RY12	0.5124
33	MRGPRD	0.8071	100	OTOF	0.6581	167	PLA2G3	0.5957	234	IMPDH1	0.5454	301	PRRG3	0.5114
34	NEFH	0.7988	101	ANGPTL7	0.6576	168	CCL1	0.5939	235	CLDN19	0.5443	302	MICALL2	0.5112
35	MRGPRE	0.7926	102	SHOX2	0.6566	169	KCND1	0.5920	236	LOC200726	0.5436	303	COL27A1	0.5110
36	P2RX3	0.7858	103	SLC18A3	0.6554	170	COL22A1	0.5899	237	FABP7	0.5431	304	SLC13A1	0.5108
37	PSMB11	0.7852	104	CALCA	0.6553	171	OR2L1P	0.5849	238	FAM90A10	0.5429	305	CHRNB3	0.5106
38	CST4	0.7728	105	PLEKHD1	0.6549	172	RDH12	0.5844	239	LOC440300	0.5426	306	FKBP1B	0.5104
39	HOXB8	0.7718	106	POU4F1	0.6519	173	FMO1	0.5841	240	MIA	0.5423	307	CCL3L3	0.5104
40	POU4F3	0.7700	107	NPPB	0.6511	174	NRG1	0.5841	241	PRG1	0.5421	308	PCBP3	0.5094
41	SNAR-B1	0.7700	108	IL31RA	0.6506	175	OR7E102P	0.5840	242	LRRC16B	0.5418	309	KCNA6	0.5091
42	SNAR-B2	0.7700	109	DEFB130	0.6499	176	LOC647012	0.5828	243	TRPV3	0.5412	310	GSTT2B	0.5084
43	FOSB	0.7584	110	LOC100133267	0.6499	177	AHNAK2	0.5827	244	VAMP1	0.5405	311	FXYD7	0.5083
44	LCTL	0.7571	111	SCN11A	0.6495	178	REEP1	0.5815	245	ISL1	0.5396	312	C2orf66	0.5082
45	TMEM132E	0.7539	112	GRIK3	0.6489	179	STMN2	0.5812	246	L1CAM	0.5396	313	OR7E59P	0.5080
46	BHLHA9	0.7505	113	FAM70A	0.6487	180	LOC100288346	0.5809	247	CHRFAM7A	0.5392	314	MOS	0.5076
47	SCGB1C1	0.7439	114	AMIGO3	0.6471	181	TSPAN11	0.5809	248	GPR83	0.5390	315	C17orf99	0.5076
48	NTRK1	0.7438	115	LOC574538	0.6467	182	CD1E	0.5802	249	LOC100129931	0.5388	316	PRSS35	0.5075
49	BARHL1	0.7424	116	OR7E130P	0.6463	183	PTPN20B	0.5801	250	AFAP1L2	0.5381	317	AURKB	0.5073
50	PRDM12	0.7422	117	TAC1	0.6449	184	HTR3A	0.5800	251	PDZD7	0.5377	318	LOC100130148	0.5067
51	FRMPD1	0.7377	118	BET3L	0.6440	185	NMB	0.5794	252	GNG3	0.5372	319	LRRTM1	0.5066
52	OR2T8	0.7376	119	SFRP4	0.6435	186	PCDH8	0.5786	253	GJC3	0.5371	320	HOXA6	0.5065
53	AVIL	0.7362	120	NEFM	0.6423	187	AQP12B	0.5781	254	CRYGD	0.5369	321	CYP1A1	0.5064
54	TRIM67	0.7359	121	POU4F2	0.6412	188	OR2A13P	0.5766	255	SNORD116-20	0.5365	322	PTPRN	0.5062
55	NBPF24	0.7344	122	MAST1	0.6374	189	HMX1	0.5754	256	RAB3D	0.5365	323	LOC100130954	0.5041
56	DRGX	0.7271	123	NGFR	0.6374	190	BTNL2	0.5754	257	CPEB1	0.5363	324	C17orf102	0.5039
57	TMEM179	0.7192	124	TUBB3	0.6367	191	ADIPOQ	0.5754	258	IFITM5	0.5358	325	C1orf130	0.5035
58	GFRA3	0.7188	125	KCNH6	0.6356	192	TMEM63C	0.5747	259	CYP2W1	0.5356	326	COL5A3	0.5035
59	NEFL	0.7183	126	VSTM5	0.6354	193	PRIMA1	0.5718	260	PODNL1	0.5344	327	FBXO2	0.5034
60	OR11H2	0.7176	127	MPZ	0.6344	194	OR7E163P	0.5713	261	KIF3C	0.5337	328	OR6B2	0.5022
61	CER1	0.7153	128	OR1H1P	0.6329	195	CHRNA7	0.5706	262	ADAMTSL1	0.5336	329	MATN2	0.5021
62	MIR570	0.7149	129	LOC149134	0.6309	196	EXTL1	0.5682	263	BCAN	0.5335	330	SLC17A6	0.5014
63	SHH	0.7125	130	AQP12A	0.6266	197	CLDN22	0.5679	264	DPYSL5	0.5313	331	CYSLTR2	0.5013
64	STAC	0.7121	131	KCTD8	0.6251	198	SCN4B	0.5672	265	HKDC1	0.5308	332	B4GALNT4	0.5008
65	MIR770	0.7100	132	TMEM233	0.6228	199	CPNE6	0.5667	266	CLEC2L	0.5298			
66	FLJ46446	0.7017	133	LOC284233	0.6224	200	SYNGR3	0.5663	267	DISP2	0.5288			
67	LOC727677	0.6995	134	TMPRSS5	0.6212	201	MIR339	0.5653	268	DHH	0.5286			

Supplementary Table 2 GPCRs expression profiling in human DRG

Rank	GPCR	DRG/All	Rank	GPCR	DRG/All	Rank	GPCR	DRG/All	Rank	GPCR	DRG/All	Rank	GPCR	DRG/All
1	GPR139	0.887	75	UTS2R	0.237	149	BAI2	0.132	223	GPRC5B	0.065	298	GPR39	0.017
2	MRGPRX4	0.886	76	HTR1B	0.235	150	HTR1F	0.131	224	GPR125	0.062	299	TSHR	0.015
3	MRGPRX1	0.829	77	CXCR3	0.235	151	P2RY11	0.131	225	ADRA2B	0.062	300	HCAR3	0.014
4	MRGPRD	0.807	78	OPRL1	0.233	152	ADORA1	0.131	226	F2R	0.060	301	RXFP1	0.012
5	MRGPRE	0.793	79	GABBR1	0.229	153	GPR45	0.129	227	GPR88	0.058	302	CHRM5	0.011
6	PROKR2	0.608	80	PTGER3	0.228	154	GPR12	0.129	228	GPR84	0.054	303	FFAR2	0.011
7	NPSR1	0.607	81	LPHN3	0.222	155	ADRA2C	0.128	229	GRM2	0.054	304	GPR182	0.010
8	FZD2	0.606	82	CELSR2	0.221	156	LPAR6	0.127	230	RHOD	0.054	305	CXCR1	0.009
9	CHRM4	0.563	83	GPR132	0.219	157	PTGER1	0.126	231	ADCYAP1R1	0.053	306	GPR97	0.008
10	LPAR3	0.562	84	GPR56	0.214	158	LPAR2	0.125	232	GPR22	0.052	307	CXCR2	0.007
11	GRM4	0.560	85	PTGER2	0.214	159	ADRB2	0.123	233	GPR135	0.052	308	F2RL3	0.006
12	F2RL2	0.556	86	GPR61	0.210	160	HTR4	0.123	234	CHRM3	0.050	309	NTSR1	0.005
13	GPR149	0.555	87	GPR64	0.209	161	ADORA2B	0.122	235	FPR1	0.050	310	GRM3	0.004
14	GPR83	0.539	88	BDKRB2	0.209	162	GPR75	0.119	236	SSTR3	0.050	311	GRM5	0.004
15	P2RY12	0.512	89	GPR142	0.208	163	TGR5	0.117	237	GPR15	0.050	312	S1PR5	0.002
16	CYSLTR2	0.501	90	P2RY1	0.207	164	CRCP	0.116	238	S1PR4	0.049	313	ADRB3	0.000
17	HTR1D	0.489	91	GPR98	0.204	165	GPR176	0.114	239	LPHN2	0.049	314	AGTR2	0.000
18	GPR114	0.487	92	PTGER4	0.199	166	NMUR1	0.114	240	OXTR	0.049	315	AVPR1B	0.000
19	GPR173	0.482	93	GPR152	0.196	167	MCHR1	0.114	241	FZD9	0.048	316	BRS3	0.000
20	CCKAR	0.478	94	HCAR1	0.194	168	GNRHR	0.112	242	GPR52	0.047	317	CCR3	0.000
21	MC5R	0.461	95	LTB4R	0.192	169	S1PR2	0.111	243	GPR113	0.047	318	CCR7	0.000
22	OPRK1	0.457	96	LPHN1	0.192	170	GPR183	0.110	244	GPR179	0.046	319	CCR8	0.000
23	GPR35	0.457	97	GPR133	0.191	171	HTR6	0.110	245	CCRL2	0.046	320	CNR2	0.000
24	FFAR1	0.447	98	P2RY6	0.188	172	FZD6	0.107	246	GPR55	0.047	321	DRD3	0.000
25	CX3CR1	0.445	99	GNRHR2	0.187	173	ADORA2A	0.104	247	ADRA1B	0.045	322	FPR2	0.000
26	FZD8	0.441	100	GPR34	0.187	174	GPR25	0.102	248	CELSR1	0.044	323	GALR3	0.000
27	GPR27	0.440	101	GPR126	0.185	175	P2RY2	0.102	249	APLNR	0.044	324	GHRHR	0.000
28	LGR5	0.436	102	RXFP3	0.184	176	GPR65	0.102	250	GRM6	0.043	325	GHSR	0.000
29	QRFPR	0.434	103	NPY5R	0.184	177	GPRC5C	0.101	251	GPR160	0.043	326	GPR101	0.000
30	GPR128	0.426	104	HTR5A	0.179	178	C5AR1	0.098	252	GIPR	0.043	327	GPR110	0.000
31	LHCGR	0.425	105	GPR153	0.179	179	FZD3	0.098	253	GPR116	0.043	328	GPR112	0.000
32	OPRD1	0.416	106	CXCR4	0.179	180	PTGIR	0.097	254	GPR141	0.043	329	GPR119	0.000
33	PTGFR	0.405	107	GPR19	0.179	181	P2RY8	0.096	255	HTR1E	0.043	330	GPR144	0.000
34	MRGPRX3	0.379	108	CRHR1	0.177	182	GPR174	0.095	256	GPR62	0.043	331	GPR148	0.000
35	MAS1L	0.378	109	CCR2	0.174	183	PTH2R	0.094	257	CCR4	0.041	332	GPR150	0.000
36	NPFFR2	0.377	110	GPR17	0.173	184	GPR3	0.093	258	NMUR2	0.041	333	GPR151	0.000
37	GPR37L1	0.373	111	GPR50	0.173	185	GPR26	0.092	259	HTR2A	0.040	334	GPR31	0.000
38	DRD2	0.368	112	CASR	0.172	186	GRM8	0.092	260	GPR123	0.039	335	GPR32	0.000
39	GPR161	0.360	113	TBXA2R	0.170	187	EMR4P	0.091	261	CHRM1	0.039	336	GPR6	0.000
40	PTGDR	0.350	114	HRH4	0.167	188	NMBR	0.090	262	GPR4	0.038	337	GPR78	0.000
41	P2RY14	0.335	115	CCR6	0.167	189	CXCR6	0.089	263	GPR21	0.037	338	GPR87	0.000
42	NPFFR1	0.329	116	AVPR2	0.167	190	TAS1R3	0.088	264	PPYR1	0.037	339	GPRC5D	0.000
43	GRM7	0.326	117	CYSLTR1	0.166	191	CCR5	0.088	265	ELTD1	0.036	340	GPRC6A	0.000
44	HRH1	0.320	118	GPR115	0.165	192	GPR77	0.087	266	EMR1	0.036	341	HCRTR1	0.000
45	CRHR2	0.317	119	CALCR	0.161	193	FZD4	0.087	267	FZD5	0.033	342	HTR1A	0.000
46	FZD1	0.313	120	GPR68	0.159	194	SSBP1	0.086	268	LTB4R2	0.033	343	KISS1R	0.000
47	SSTR4	0.311	121	TRIM5	0.158	195	CCRL1	0.085	269	HCAR2	0.032	344	LPAR4	0.000
48	GPR124	0.305	122	TACR1	0.157	196	DRD1	0.085	270	CALCRL	0.032	345	MC2R	0.000
49	BAI1	0.304	123	O3FAR1	0.157	197	MC4R	0.083	271	F2RL1	0.032	346	MC3R	0.000
50	CCR10	0.304	124	CCKBR	0.156	198	SSTR2	0.082	272	AVPR1A	0.031	347	MCHR2	0.000
51	LPAR5	0.298	125	HRH3	0.156	199	GPR162	0.082	273	GPR37	0.028	348	MLNR	0.000
52	LPAR1	0.294	126	GLP1R	0.156	200	MTNR1A	0.081	274	S1PR1	0.028	349	MRGPRG	0.000
53	DRD4	0.293	127	GPR82	0.155	201	CCBP2	0.080	275	TACR2	0.028	350	MRGPRX2	0.000
54	PROKR1	0.291	128	GPR20	0.155	202	CCR1	0.080	276	SUCNR1	0.027	351	MTNR1B	0.000
55	BAI3	0.288	129	CMKLR1	0.154	203	HRH2	0.079	277	GPR1	0.026	352	NPBWR1	0.000
56	ADRA1D	0.287	130	CXCR7	0.151	204	BDKRB1	0.078	278	CHRM2	0.025	353	NPBWR2	0.000
57	GALR1	0.285	131	C3AR1	0.150	205	DARC	0.077	279	GRM1	0.025	354	NPY2R	0.000
58	FZD7	0.282	132	S1PR3	0.149	206	GPR111	0.076	280	HTR2C	0.025	355	OPN5	0.000
59	GPR156	0.281	133	GPR85	0.147	207	ADORA3	0.075	281	LGR6	0.024	356	P2RY10	0.000
60	P2RY13	0.274	134	PTAFR	0.147	208	OXGR1	0.073	282	EMR3	0.024	357	PRLHR	0.000
61	CCR9	0.273	135	Tpra1	0.147	209	GRPR	0.072	283	GPR18	0.024	358	RXFP2	0.000
62	SMO	0.270	136	NPY1R	0.144	210	MRGPRF	0.072	284	GLP2R	0.024	359	RXFP4	0.000
63	P2RY4	0.266	137	OXER1	0.143	211	HCRTR2	0.071	285	AGTR1	0.024	360	SSTR5	0.000
64	GABBR2	0.262	138	OPN3	0.143	212	CNR1	0.070	286	FSHR	0.023	361	TAAR3	0.000
65	FZD10	0.260	139	Gpr137	0.142	213	MAS1	0.070	287	Gpr143	0.023	362	TAAR5	0.000
66	EDNRB	0.259	140	EDNRA	0.140	214	OPRM1	0.070	288	ADRB1	0.023	363	TAAR6	0.000
67	MC1R	0.258	141	GPR157	0.140	215	C17orf103	0.070	289	VIPR1	0.023	364	TAAR8	0.000
68	CELSR3	0.257	142	GPR146	0.139	216	CD97	0.070	290	VIPR2	0.022	365	TACR3	0.000
69	ADRA2A	0.252	143	GPER	0.137	217	NTSR2	0.067	291	HTR2B	0.021	366	TAS1R2	0.000
70	DRD5	0.249	144	GPR63	0.136	218	FFAR3	0.066	292	CXCR5	0.020	367	TRHR	0.000
71	LGR4	0.242	145	TAS1R1	0.134	219	SCTR	0.066	293	ADRA1A	0.019	368	XCR1	0.000
72	HTR7	0.241	146	NPY6R	0.134	220	SSTR1	0.066	294	GPRC5A	0.018			
73	GPR158	0.240	147	PTH1R	0.134	221	EMR2	0.066	295	GALR2	0.018			
74	Gpr107	0.240	148	FPR3	0.133	222	GCGR	0.065	296	GPR171	0.017			